JFH1 transfection led us to suspect the occurrence of CPE, produced in host cells by HCV infection and replication. A plaque assay was performed (see Materials and methods) to investigate the morphological CPE following HCV-JFH1 infection. Culture supernatants from JFH1-transfected cells were diluted serially and inoculated onto uninfected Huh-7.5.1

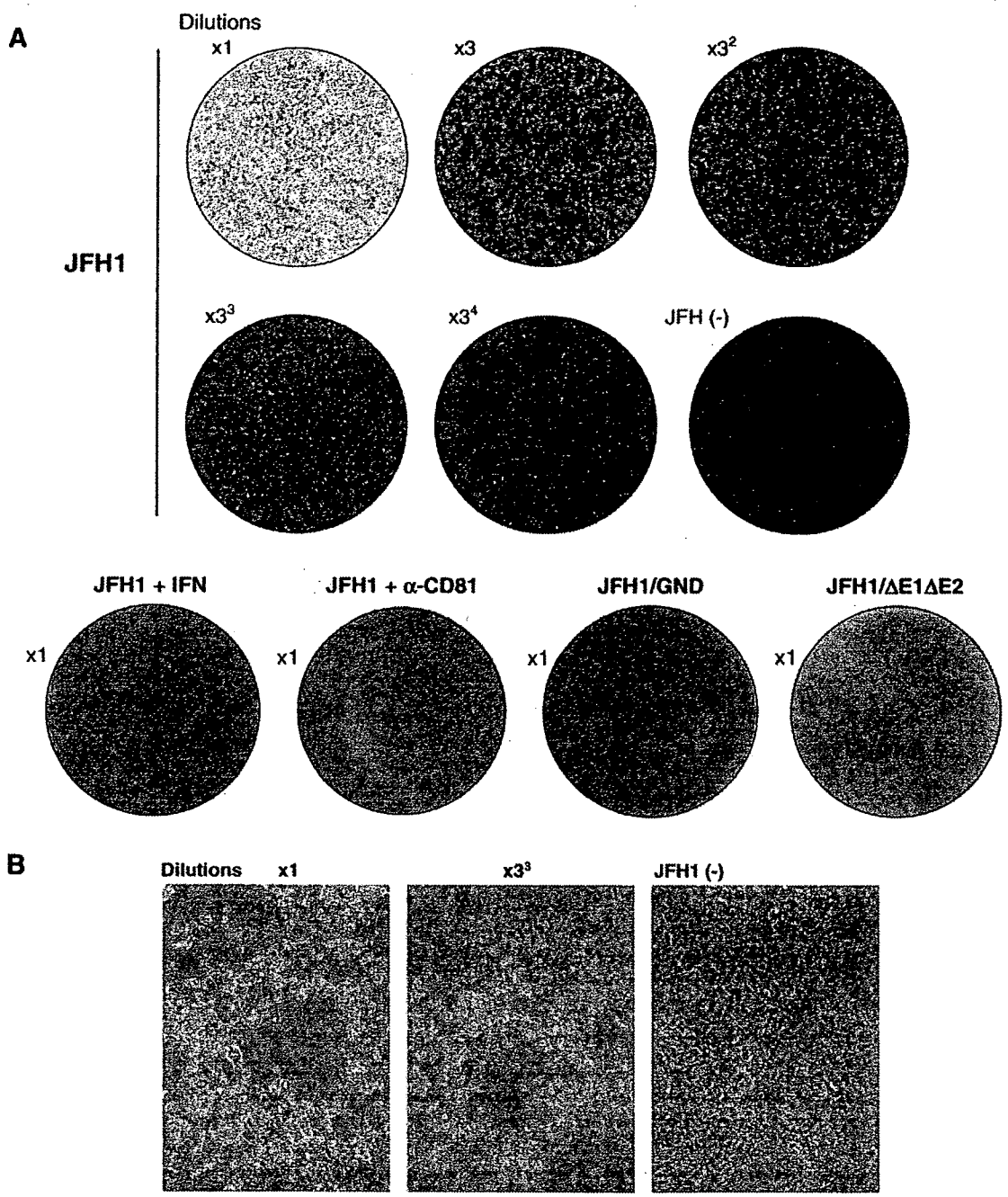

Fig. 2. The cytopathic effects of HCV-JFH1 *in vitro*. (A) Plaque assay. Upper panel, Huh-7.5.1 cells were seeded in collagen-coated 60-mm-diameter plates at density of 4×10^5 cells per plates and were incubated at 37 °C under 5.0% CO_2 (as described above). After overnight incubation, HCV-infected culture supernatants were serially diluted in a final volume of 2 ml per plates and transferred onto the cell monolayers. After ~5 h of incubation, the inocula were removed and the infected cells were overlaid with 8 ml of culture medium containing 0.8% methylcellulose and incubated under normal conditions. After 7 days culture, formation of cytopathic plaque was visualized by staining with 0.08% crystal violet solution. Lower panel, JFH1 + IFN; after infection of the virus supernatant, the cells were cultured in the presence of 50 U/ml interferon-alpha. JFH1 + a-CD81, Huh-7.5.1 cells were pretreated with 10 μg/plate of anti-CD81 antibody. After incubation at 37 °C for 30 min, anti-CD81 was removed, the cells were washed with PBS, and the HCV-JFH1 culture supernatant was transferred. After ~5 h incubation, the supernatant was removed and the infected cells were overlaid with 8 ml of culture medium containing 0.8% methylcellulose and controls for the plaque assay were also performed with the JFH1/GND or JFH1/ΔE1-E2 culture supernatant. (B) The cytopathic plaques were observed by phase-contrast microscopy at day 7 after HCV-JFH1 infection.

cells. The cells were subsequently cultured in medium containing agarose. Almost 10 days after the inoculation, viable cells were stained and plaques were visualized (Fig. 2A, upper panel). HCV-inoculated cell cultures developed plaques as unstained areas that were accompanied by round cells in the periphery (Fig. 2B). The formation of cytopathic plaques was not observed in a parental Huh7 cell line (data not shown). Immunocytochemistry of the foci revealed the presence of HCV core-positive cells surrounding the cytopathic plaques (Fig. 3A). Culture of the HCV-inoculated cells in the presence of interferon-alpha (50 U/ml) completely abolished the formation of plaques (Fig. 2A, lower panel). Uninfected Huh-7.5.1 cells (Fig. 2A, upper panel), Huh-7.5.1 cells treated with anti-CD81 antibody before HCV-JFH1 infection and JFH1/GND or JFH1/ΔE1-E2-transfected cell cultures did not develop plaques (Fig. 2A, lower panel). These findings suggest that HCV-infected cells develop cytopathic plaques depending on the quantity of the inoculums and that HCV replication, viral protein expression and the propagation of viral particles were the features of these plaques.

HCV-JFH1 infection induced host-cell apoptosis

We next determined whether the cytopathic effects of HCV-JFH1 replication include process of apoptotic cell death. Cells including plaques were double-stained with annexin V-FITC and PI. The ligand of annexin V, phosphatidylserine, is normally confined to the cytoplasmic leaflets of the plasma membrane. In the early phase of apoptosis, phosphatidylserine is exposed on the outer surface of the plasma membrane, which enables detection of FITC-labeled annexin V. As shown in Fig. 4, the fluorescence of annexin V was observed in the cells around the plaques. Foci of apoptotic cells were scattered in the plaques. On the other hand, the expression of annexin V was slightly detectable in the subgenomic replicon-harboring cells, though they were at the same level as the uninfected Huh-7.5.1 cells and the cell death was not observed. Therefore, the cells that express HCV subgenomic replicons did not induce apoptotic cell death. These findings demonstrate that the cytopathic effects of HCV replication and the particle formation induce apoptotic cell death.

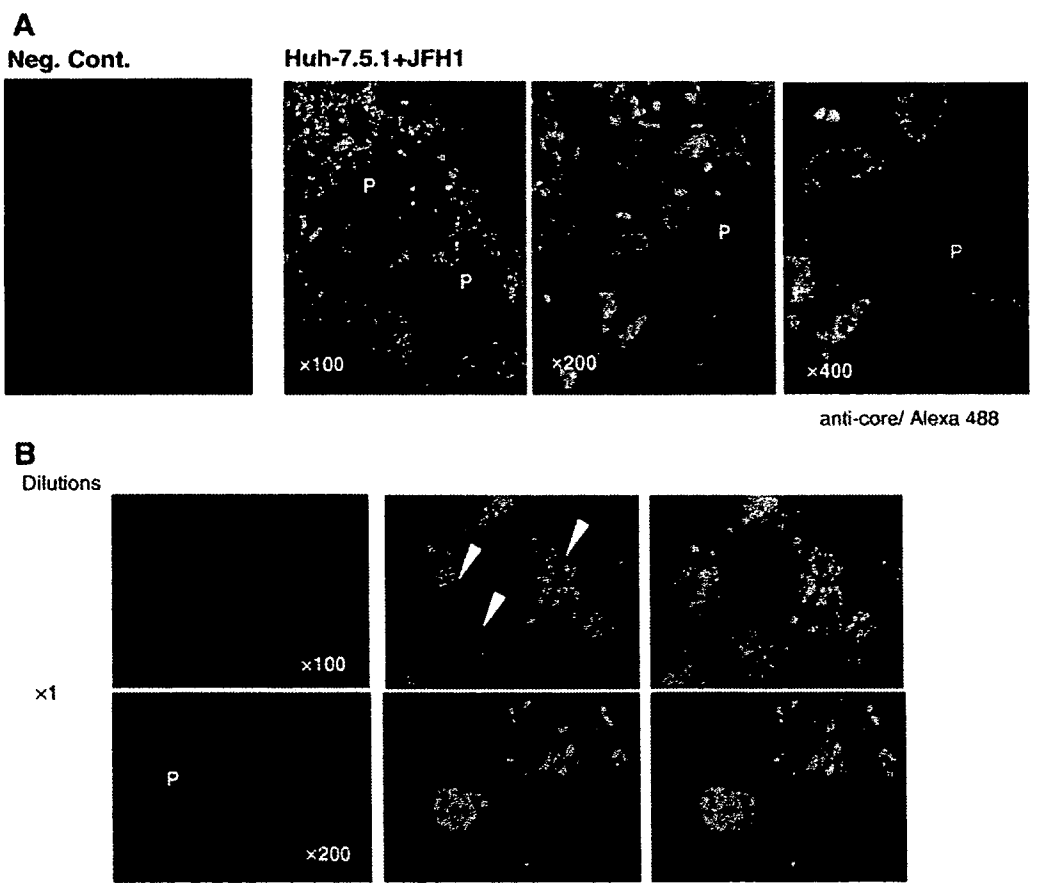

Fig. 3. Immunofluorescence detection of HCV core protein in cytopathic plaques. (A) The HCV-JFH1 culture supernatant was transferred onto uninfected Huh-7.5.1 cells, plated on 22 mm-round micro cover glasses in 60-mm-diameter plates at density of 2×10^5 cells per plate. After ~5 h incubation, the supernatant was replaced with medium containing 0.8% methylcellulose. Immunocytochemistry was performed 12 days after infection. A 'P' indicates a cytopathic plaque. (B) Immunofluorescence detection of HCV-positive foci and cytopathic plaques. The HCV-JFH1 culture supernatant was transferred at various dilutions onto uninfected Huh-7.5.1 cells. After ~5 h incubation, the supernatant was removed and the infected cells were cultured in 60-mm-diameter plate with medium containing 0.8% methylcellulose. Immunocytochemistry was performed 5 days after infection using mouse anti-core antibody. The infectivity and cytotoxicity were quantified by counting HCV-positive foci (FFU/ml) and cytopathic plaque (PFU/ml) respectively. White arrowheads indicate HCV-positive foci.

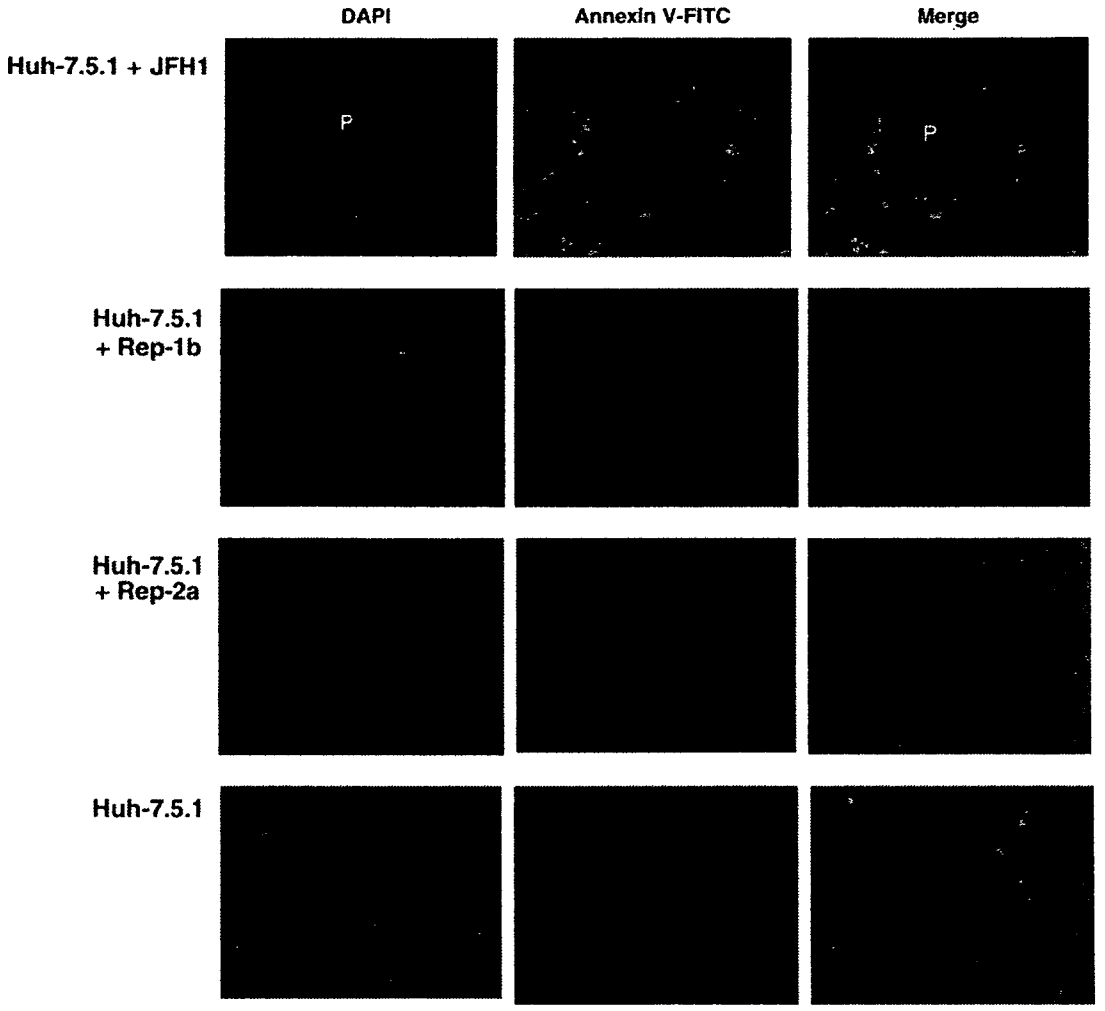

Fig. 4. HCV-JFH1 infection induces apoptosis and leads to plaque formation. The HCV-JFH1 culture supernatant was transferred onto uninfected Huh-7.5.1 cells plated on 22-mm round micro cover glasses in 60-mm-diameter plates at density of 2×10^5 cells per plate. After ~5 h incubation, the supernatant was replaced with medium containing 0.8% methylcellulose. Thirteen days after infection, cover glasses were incubated with 100 μl of staining solution containing Annexin V-FITC at room temperature for 10 to 15 min. The cells that express HCV subgenomic replicons were also incubated and stained with Annexin V-FITC. Rep 1b, Rep-Feo; Rep 2a, SGR-JFH1 (see Materials and methods).

JFH1 replication activates expression of ER stress-related proteins

Cellular stresses such as virus infections prevent protein folding and maturation in the endoplasmic reticulum (ER) and result in the accumulation of misfolded proteins (ER stress) (Kaufman, 1999; Pahl, 1999), triggering the unfolded protein response (UPR). The UPR leads to global shut-off of protein translation and to apoptotic cell death (Ferri and Kroemer, 2001; Mori, 2000; Munro and Pelham, 1986). We and other groups have previously reported that subgenomic or genomic HCV replication induces ER stress and triggers UPR (Nakagawa et al., 2005; Tardif et al., 2002). Therefore, we next studied expression of the ER stress-related proteins, GRP78 and phosphorylated eIF2-alpha, in JFH1-infected cells (Fig. 5). GRP78 is one of the ER chaperones whose expression is induced by ER stress through cleavage and nuclear translocation of ATF6. The eIF2-alpha is phosphorylated by PER-like ER kinase (PERK) on ER stress, causing direct global inhibition of initiation of protein translation (Harding et al., 1999). Huh-7.5.1 cells were infected with HCV-JFH1 supernatant and harvested on the fourth and seventh days post-infection (Fig. 5). As the expression of HCV core protein increased, expression levels of GRP78 and phosphorylated eIF2-alpha also increased substantially. Suppression of virus replication by interferon-alpha treatment led to a decrease of cellular GRP78 and phosphorylated eIF2-alpha. Interferon-alpha treatment did not eliminate the expression of HCV completely, though the levels of core and phosphorylated eIF2-alpha expression apparently decreased compared with the JFH-1 infected Huh-7.5.1 cells at seventh days post-infection. These findings demonstrated that HCV-JFH1 infection induced ER stress.

Persistence of ER stress activates apoptosis signaling pathways, including the induction of C/EBP homologous protein (CHOP) and activation of JNK kinase and caspase12, leading to cell death (Ferri and Kroemer, 2001). As shown in Fig. 5, the

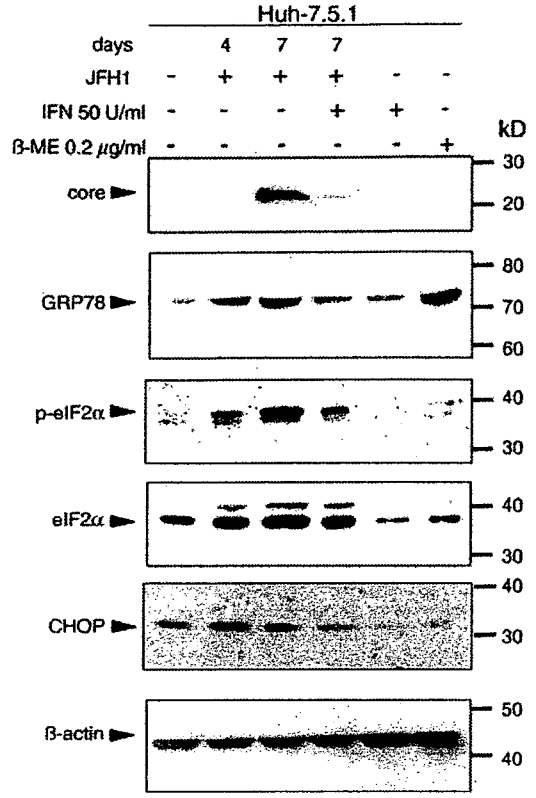

Fig. 5. Expression of ER stress-related proteins in HCV-JFH1 infected cells. The supernatant of JFH1-transfected Huh-7.5.1 cells was transferred onto uninfected Huh-7.5.1 cells. The cells were harvested at 4 and 7 days after infection. The JFH1-infected cells were also cultured with interferon (50 U/ml) or 2-mercaptoethanol (0.2 μg/ml) and harvested after 48 h after treatment. 2-Mercaptoethanol was used as a positive control to induce ER stress (Nakagawa et al., 2005). Western blotting was performed using anti-core, anti-GRP78, anti-phospho-eIF2-alpha (p-eIF2α), anti-eIF2-alpha, anti-GADD153/CHOP, and anti-beta-actin antibodies. β-ME, 2-mercaptoethanol.

level of CHOP expression was apparently increased in JFH1-infected Huh-7.5.1 cells.

To determine whether ER stress contributes to the formation of cytopathic plaques, JFH1-infected cells were incubated in methylcellulose-containing medium and double immunofluorescence staining of the plaques was performed. As shown in Fig. 6, overexpression of GRP78 was colocalized with HCV-core-positive cells with and without CPE. Together with the result shown in Fig. 4, these findings suggest that ER stress is induced in the HCV-JFH1-infected cells and these responses may be involved in development of apoptosis and the formation of cytopathic plaques.

A cytopathic clone could be isolated and this had acquired a high infection efficiency and increased cytopathogenicity

The plaque assay enabled differential quantification of viral infectivity and cytopathogenicity by the immunofluorescence detection of HCV core protein in JFH1-infected, plaque-developed cultures. The number of plaques, as well as infectious foci, was linearly proportional to the dilution of an inoculum (Fig. 7B). It was revealed that only a few populations of HCV-positive foci developed cytopathic plaques (Fig. 3B and Table 1). The infectious focus-forming units and plaque-forming units were 5.6×10^3 FFU/ml and 9.7×10^2 PFU/ml, respectively (Table 1).

To determine whether the difference between the cytopathic and noncytopathic HCV-JFH1 replication might be attributable to viral factors, we isolated clones from each cytopathic plaque. JFH1-infected Huh-7.5.1 cells were incubated in DMEM containing methylcellulose. Cytopathic plaques became visible at ~1 week after inoculation. We isolated cells from each plaque using a cloning cylinder, subcultured, and transferred supernatant onto uninfected Huh-7.5.1 cells. To our surprise, infection of naive cells with plaque-derived supernatants led to massive cell death at 10 days post-infection (Fig. 8A). The supernatant of these cells was transferred again onto uninfected Huh-7.5.1 cells again. Immunofluorescence assay revealed that almost 100% of the cells were positive for HCV core protein (Fig. 8B). The infectivity and cytopathogenicity of this isolated plaque (Pl #1) were 4.9×10^3 FFU/ml and 3.0×10^3 PFU/ml respectively (Table 1), much higher than the parental JFH1 clone. Moreover, the ratio of PFU to FFU in a plaque-isolated clone (Pl #1) was significantly higher than that of parental JFH1 clone (0.58 and 0.17 respectively) (Table 1 and Figs. 7B and C). We next performed an infection experiment of the parental JFH1 and a plaque-derived clone by adjusting infectious titers of the inocula by HCV core antigen levels. As shown in Fig. 8C, virus from cytopathic plaque (Pl #1, #2, #3) showed significantly higher elevation of core antigen levels in supernatants than the parental JFH1 in every time point. The second round isolation of plaques from the Pl #1 subclone (Pl #1-1, #1-2 and #1-3 in the Table 3) showed consistently higher replication efficiency and cytopathogenicity. These results indicated that JFH1 subclones isolated from cytopathic plaques showed significantly higher infection efficiency and greater cytopathic effects than the original JFH1.

The isolated plaque had amino acid substitutions clustered in the NS5B region

To determine whether there are viral mutations in the cytopathic JFH1 subclone (Pl #1), we performed sequence analyses. As shown in Table 2, 11 nucleotide changes were found in the cytopathic plaque, and 9 of these were non-synonymous mutations (81.8%). In particular, 6 of the 11 mutations (9153, 9232, 9293, 9295, 9353, and 9355) were clustered in the C terminal half of the NS5B region. We also performed sequence analyses of the Pl #1-isolated subclones, Pl #1-1, #1-2, and #1-3, and other clones that had been independently isolated from different plaques, Pl #2, #3, and #4 (Table 3). Those subclones showed similar mutations within NS5B region. The C2438S, P2934S, and S3001N substitutions were redundantly appeared in the 4 plaque-isolated clones and in all three Pl #1-derived subclones. In contrast, no mutations were found in the virus from infectious foci without plaque formation. These results showed an evidence that certain amino acid mutations were directly associated with the viral replication efficiency and cytopathogenicity.

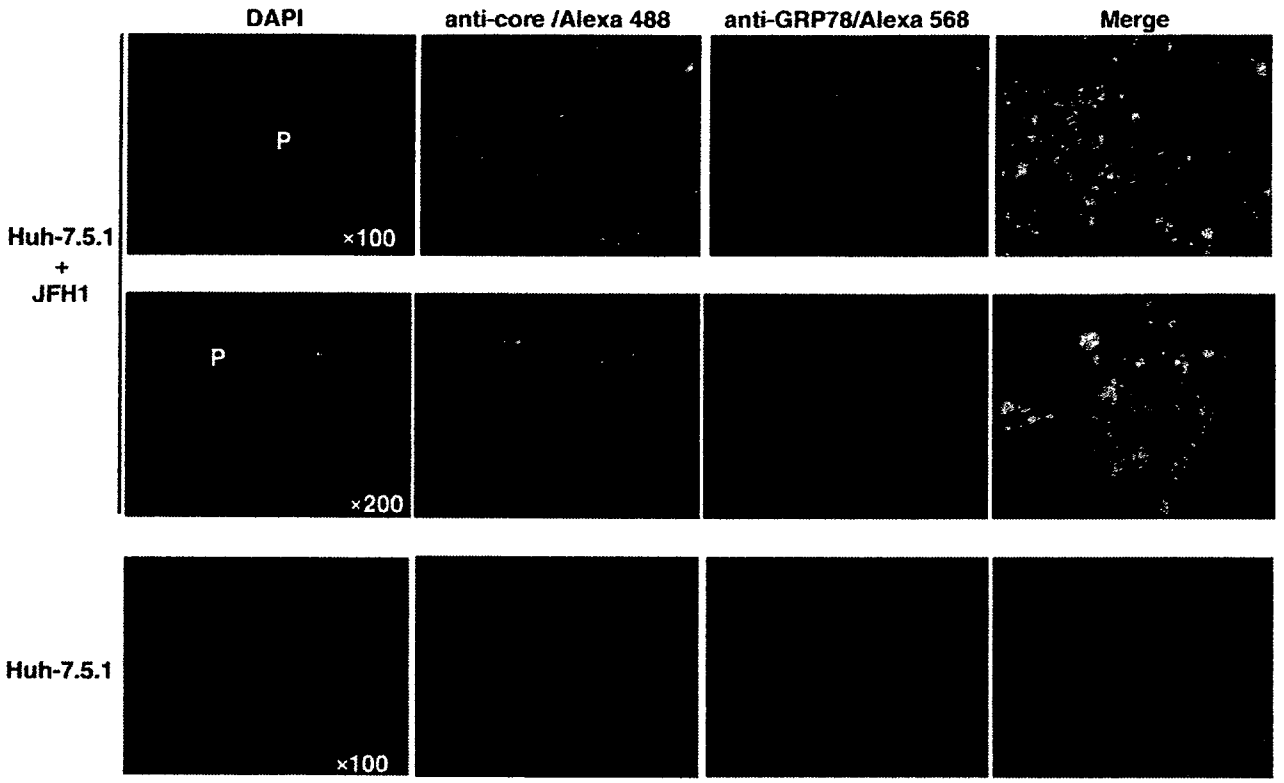

Fig. 6. Co-expression of HCV core and GRP78 in the cytopathic plaque. The HCV-JFH1 culture supernatant was transferred onto uninfected Huh-7.5.1 cells plated on 22-mm round micro cover glasses in 60-mm-diameter plates at density of 4×10^5 cells per plate. After ~5 h incubation, the supernatant was replaced with medium containing 0.8% methylcellulose. Double immunofluorescence was performed 10 days after infection using mouse anti-core antibody and goat-anti-GRP78 antibody.

Introduction of NS5B mutations in JFH1 clone showed higher replication efficiency and cytopathogenicity

We finally investigated on phenotypes of the amino acid mutations identified in the isolated cytopathic subclones. We constructed mutant clones from the wild type JFH1 plasmid, in which three amino acid mutations in NS5B region were individually introduced; T7662A, C9153T, and G9295C (see Tables 2 and 3). Transfection of the mutant HCV-RNAs showed that all mutants developed massive cell death on 10 days after transfection and that their extents of the CPE were apparently greater than the wild type JFH1 clone (Fig. 9A). The levels of core antigen in the culture medium were significantly higher in the mutant clones than in the wild type (Fig. 9B). Furthermore, the expression levels of cellular HCV core protein were significantly higher in the mutant clones than in the wild type with the order of T7662>C9153≫G9295C>JFH1 (Fig. 9C).

Discussions

Our results show that replication of HCV-JFH1 resulted in morphologic changes to the host cells, which are characterized by massive cell death (Figs. 1–3). These observations suggested that HCV infection and replication could cause CPE on the host cells. The development of the CPE involved virus protein-induced ER stress and subsequent apoptotic cell death (Figs. 4–6). The JFH1/ΔE1-E2 with deletion of the HCV envelope proteins-infected Huh-7.5.1 cells did not induce the CPE (Fig. 2A), which indicates that the key factors of plaque formation are not only viral replication but also the propagation of virus particles and re-infection. We took advantage of the HCV-induced CPE and developed a plaque assay using highly permissive Huh-7.5.1 cells. The assay revealed that the HCV-induced cytopathogenicity varied between infectious foci with cytopathic and noncytopathic infection (Fig. 3B). Interestingly, isolated JFH1 subclones from the plaques showed significantly increased infectivity and cytopathogenicity (Table 1 and Fig. 8). Viral genetic analyses showed nine amino acid substitutions; among them five were clustered in the C terminal half of the NS5B region, which might contribute to virus replication efficiency and cytopathogenicity (Table 2).

Cytopathic effects are key characteristics of the *Flaviviridae* that include Japanese encephalitis virus (JEV) (Vaughn and Hoke, 1992), West Nile Virus (Borisevich et al., 2006), yellow fever virus (Quaresma et al., 2006), dengue virus (DEN) (Despres et al., 1993), and bovine viral diarrhea virus (BVDV) (Mendez et al., 1998) and also of viruses such as adenovirus (Shinoura et al., 1999), Epstein–Barr virus (Sato et al., 1989), poliovirus (Yanagiya et al., 2005), and influenza virus (Hinshaw et al., 1994). The *Flaviviridae* utilizes the ER as the primary site for genomic replication and protein synthesis (Jordan et al., 2002; Su et al., 2002; Tardif et al., 2004). It has been reported that apoptotic cell death mediated by virus-induced ER stress contributes to the cytotoxicity of JEV, BVDV, and DEN-2

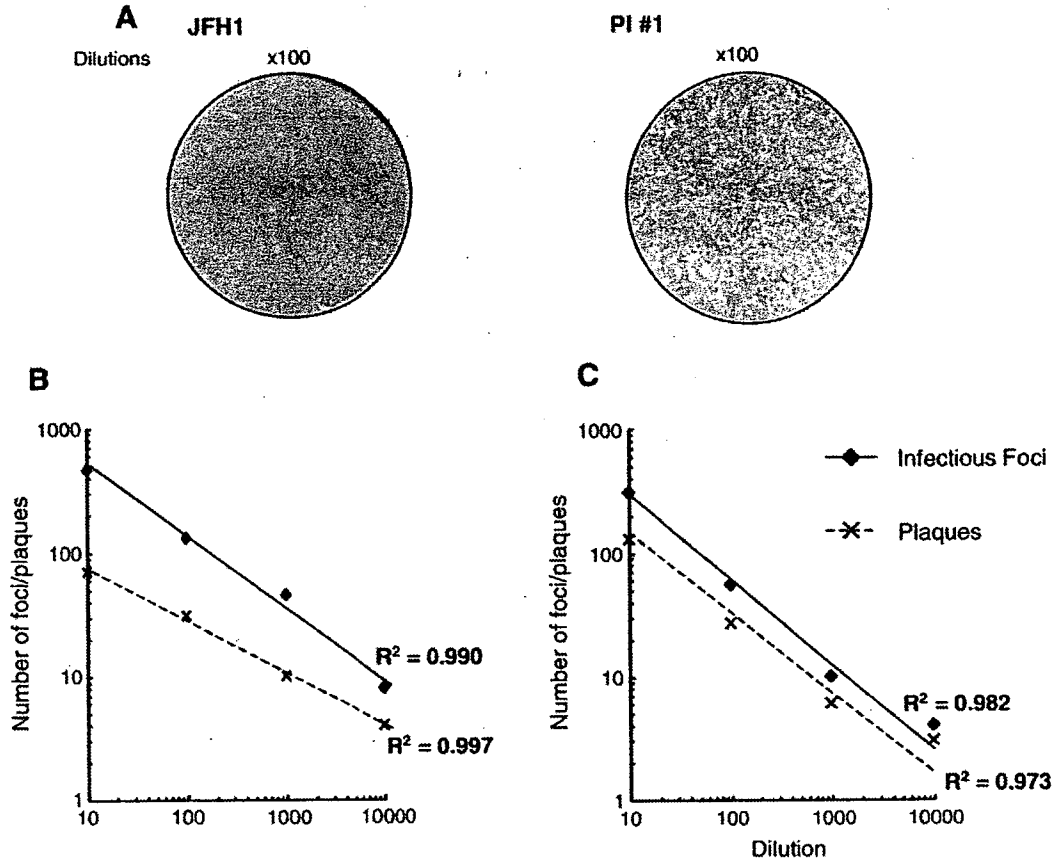

Fig. 7. Correlation of infectious foci or plaques with dilution of an inoculum. (A) Plaque assay. Huh-7.5.1 cells were seeded in collagen-coated 60-mm-diameter plates at density of 4×10^5 cells per plates and were incubated at 37 °C under 5.0% CO_2. After overnight incubation, HCV-JFH1 (left panel) or plaque-purified clone (PI #1) (right panel) infected culture supernatants were serially diluted in a final volume of 2 ml per plates and transferred onto the cell monolayers. After ~5 h of incubation, the inocula were removed, and the cell monolayers were overlaid with 8 ml of culture medium containing 0.8% methylcellulose. After 7 days of culture under normal conditions, formation of cytopathic plaque was visualized by staining with 0.08% crystal violet. (B and C) The PFU-adjusted culture supernatant of parental HCV-JFH1 (B) or plaque-purified clone (PI #1) (C) was transferred at various dilutions onto uninfected Huh-7.5.1 cells, and the plaque assay and immunocytochemistry were performed (described above). The infectivity and cytotoxicity were quantified by counting HCV-positive foci and cytopathic plaque respectively. The horizontal axis showed dilutions of the viral supernatant and the vertical axis showed the number of infectious foci or plaques.

(Jordan et al., 2002; Su et al., 2002; Yu et al., 2006). In DEN-2-infected cells, the NS2B-3 protein causes XBP1 splicing and induces ER stress (Yu et al., 2006). These findings are consistent with our results for HCV in that the JFH1 infection induced ER stress and unfolded protein responses and led to apoptotic cell death and formation of plaques.

The ER is closely associated with viral replication and assembly. Most of the HCV structural and nonstructural proteins accumulate in the ER membrane and form a membranous web that is characterized by a convoluted ER structure (Gosert et al., 2003). Moreover, the folding and assembly of HCV proteins require interaction with ER chaperone proteins such as calreticulin, BiP/GRP78, and heat shock protein-90 (HSP90) (Choukhi et al., 1998; Waxman et al., 2001). The ER stress, which is induced by virus replication, involves three different mechanisms (Tardif et al., 2002): transcriptional induction, translational attenuation, and protein degradation. In our study, both GRP78 and phosphorylated eIF2-alpha proteins were induced as viral proteins increased in concentration in HCV-JFH1 infected cells, and the GRP78 or annexin V and HCV core proteins co-localize in cytopathic plaques, showing that HCV infection and replication induce UPR and that ER stress-mediated apoptosis causes the viral cytopathic effects on host cells.

Several HCV structural and nonstructural proteins are involved in the ER stress. The structural glycoproteins, E1 and E2, interact with ER chaperones (Choukhi et al., 1998; Liberman et al., 1999), HCV NS4B induces UPR through ATF6 or the IRE1-XBP1 pathway (Zheng et al., 2005), and HCV core triggers apoptosis by inducing ER stress and ER calcium depletion both *in vitro* and *in vivo* (Benali-Furet et al., 2005).

Table 1
Cytopathogenicity and infectivity of JFH1 clones

	PFU/ml[a]	FFU/ml[b]	PFU/FFU
JFH1	$9.7 \pm 3.8 \times 10^{2}$[c]	$5.6 \pm 0.9 \times 10^{3}$	0.17±0.05
PI #1	$3.0 \pm 1.9 \times 10^{3}$	$4.9 \pm 1.6 \times 10^{3}$	0.58±0.21

[a] PFU, plaque-forming unit.
[b] FFU, focus-forming unit.
[c] Values are displayed as mean±S.D.

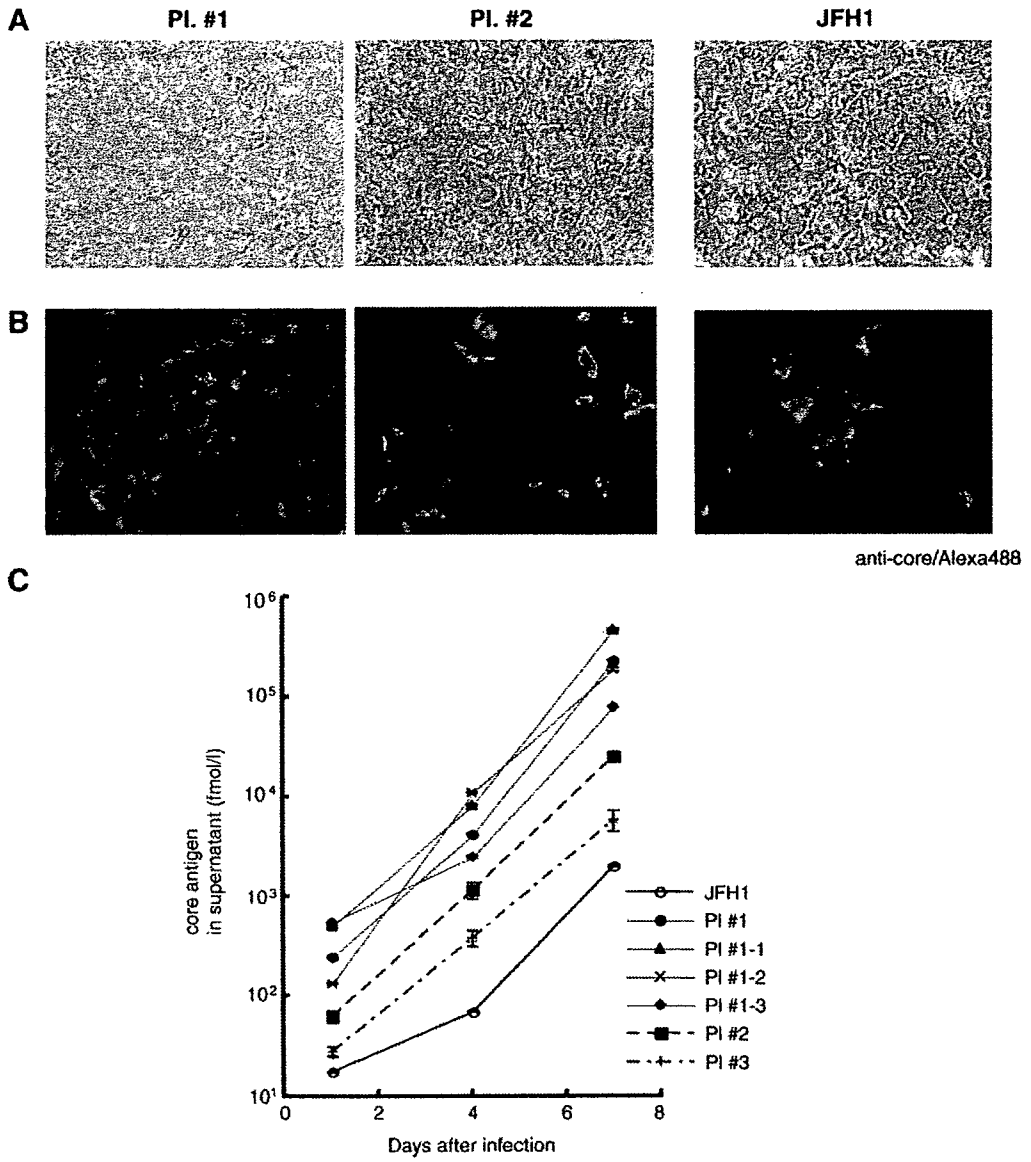

Fig. 8. The isolation of cytopathic plaques. The HCV-JFH1 culture supernatant was transferred at various dilutions onto uninfected Huh-7.5.1 cells. After ~ 5 h incubation, the supernatant was removed then infected cells were cultured in 0.8% methylcellulose-containing medium in 60-mm-diameter plates. Cytopathic plaques were detectable at 8 days after infection. Cells from each plaque were isolated using a cloning cylinder, subcultured, and transferred onto uninfected Huh-7.5.1 cells. (A) Observation by phase-contrast microscopy at 10 days of culture. (B) After 15 days of culture, the supernatant was transferred onto uninfected Huh-7.5.1 cells and an immunofluorescence assay was performed 5 days after infection using anti-core antibody. (C) Supernatants from parental JFH1, plaque-derived viruses (Pl #1, #2, and #3) and the second round isolation of plaques from the Pl #1 subclones (Pl #1-1, #1-2, and #1-3) were inoculated onto Huh-7.5.1 cells with PFU-adjusted doses, respectively. HCV core antigen levels in culture medium were measured on the days indicated. Inoculation and the assays were done in triplicate. The S.D.s were within 4% in each plot.

HCV E2 induces ER stress at lower levels but binds to PERK and inhibits phosphorylation of eIF2-alpha at high levels of expression (Pavio et al., 2003). These reports have shown that HCV may induce ER stress and regulate subsequent intracellular responses to promote its survival in hepatocytes. Consistently with these reports, our findings that HCV-JFH1 induces the expression of an ER chaperon protein and phosphorylation of eIF2-alpha indicates that robust replication of HCV-JFH1 produces unfolded proteins in the ER, leading to activation of ATF6 and stimulation of the transcription of ER chaperon proteins to promote protein folding. HCV-JFH1-induced unfolded proteins also activate PERK, which phosphorylates eIF2-alpha to inhibit the protein translation. Furthermore, the severe ER stress finally activates apoptosis signaling pathways at the early stage of viral infection. Although which HCV-JFH1 gene product is involved in ER stress-mediated apoptosis is not identified in our study, such proteins may contribute to the regulation of ER stress signaling in the host cell that leads to viral survival or cell death.

The plaque assay is often used to quantify virus infectious titers by visualizing the viral-induced CPE. However, due to the noncytopathic nature of HCV and the lack of highly permissive

Table 2
Nucleotide changes and amino acid substitutions in the cytopathic JFH1 subclone

Nucleotide[a]	Amino acid[a]
A1353G	M334V
C2842A	T843K
G3402A	G1017S
A5819G	Synonymous
T7662A	C2438S
C9153T	P2934S
G9232A	G2960D
G9293C	Synonymous
G9295C	R2985P
C9353A	H3000Q
G9355A	S3001N

[a] Nucleotide and amino acid numbers were derived from pJFH1full (Wakita et al., 2005).

host cell lines, detection of HCV-infected cells commonly relied on visualization of the infected focus by immunostaining HCV proteins (Zhong et al., 2005). Disadvantages include the costs of the antibodies and substrate, additional steps for assay and detection, and microscopic examination to count the foci. By using a highly permissive host cell line and optimizing several conditions, we have developed a plaque assay for HCV. Because the HCV-JFH1 strain is not absolutely cytopathic and does not kill all infected cells, the calculated plaque-forming units do not directly reflect HCV infectious titer but rather reflect cytopathogenicity or the percentage of cytopathic clones in the total infectious foci.

The HCV plaque assay revealed that JFH1 infection and replication developed cytopathic and noncytopathic infectious cell foci (Fig. 3B). One would suspect that the different outcomes of HCV replication might be attributable to the clonal heterogeneity of the host cells. However, there are several pieces of evidence that the Huh-7.5.1 cell line, which we used as host, might be a homogenous cell line. Huh-7.5.1 is derived from parental Huh7 cells through two rounds of clonal selection for neomycin resistance that were dependent on permissiveness for the HCV subgenomic replicon (Blight et al., 2002; Zhong et al., 2005). Sumpter et al. have reported that the HCV-permissive feature is due to mutational inactivation of RIG-I, a cytoplasmic double-stranded RNA sensor that induces type-I IFN production (Sumpter et al., 2005). This evidence suggests that the cytopathic HCV replication is attributable to virus factors, in particular, virus genomic alteration and not by clonal variation or evolution of the host cells.

Indeed, the isolation of the plaque-forming HCV subclones and inoculation onto naive cells showed significantly higher replication yields (Fig. 8) and more frequent development of cytopathic plaques (Table 1). These findings indicate that HCV-JFH1 has evolved into cytopathic and noncytopathic subclones. Our results are similar to BVDV infection. BVDV is divided into two biotypes, cytopathic (*cp*) and noncytopathic (*ncp*) strains. Most *cp* strains, which induce strong apoptotic cell death upon infection, develop from the *ncp* strains by RNA recombination such as insertion of cellular sequences, duplications and rearrangements, and deletions and lead to expression of the NS3 protein (Meyers and Thiel, 1996). Kummerer et al. have reported that other *cp* strain had point mutations in NS2 that enhanced cleavage of NS2/3 junction and NS3 production (Kummerer and Meyers, 2000). As for HCV, considering a rapid HCV replication cycle and the poor fidelity of the viral NS5B RNA-dependent RNA polymerase (RdRp) (Bartenschlager and Lohmann, 2000; Kato et al., 2005), evolution of sequence variants may well develop even after a transfection of cloned HCV-RNA. Very recently, *in vitro* permissive subclones of HCV genotype 1a, H77S stain, have been reported, which have five cell culture-adaptive mutations in the NS3, 4A, and 5A regions (Yi et al., 2007). In these clones, introduction of amino acid substitutions in the p7 and NS2 region enhanced production of the virion particles.

Interestingly, sequence analyses of a cytopathic HCV-JFH1 subclone (Pl #1) identified six amino acid substitutions in the NS5B RdRp (Table 2). Three of the six mutations were redundantly appeared in other clones that were independently isolated from the plaques (Table 3). These findings make us speculate that these amino acid substitutions may affect the enzymatic activity of RdRp by altering tertiary structure of the

Table 3
Nucleotide changes and amino acid substitutions in the NS5B regions of the cytopathic JFH1 subclones

Pl #1	#1-1	#1-2	#1-3	Pl #2	Pl #3	Pl #4
						T7623A (S2428T)
T7662A (C2438S)	T7662A (C2438S)	T7662A (C2438S)	T7662A (C2438S)	T7662A (C2438S)	T7662A (C2438S) A7550C C7551A (N2470T)	
						G8259C C8260G (A2640R)
C9153T (P2934S)	C9153T (P2934S)	C9153T (P2934S)	C9153T (P2934S)		C9153T (P2934S)	
				G9162T (V2941L)		
					A9201T (I2954F)	
G9232A (G2960D)						
				G9235A (R2965Q)		
G9295C (R2985P)	G9295C (R2985P)		G9295C (R2985P)			
C9353A (H3000Q)	C9353A (H3000Q)					
G9355A (S3001N)	G9355A (S3001N)		G9355A (S3001N)			G9355A (S3001N)

Nucleotide and amino acid numbers were derived from pJFH1full (Wakita et al., 2005).

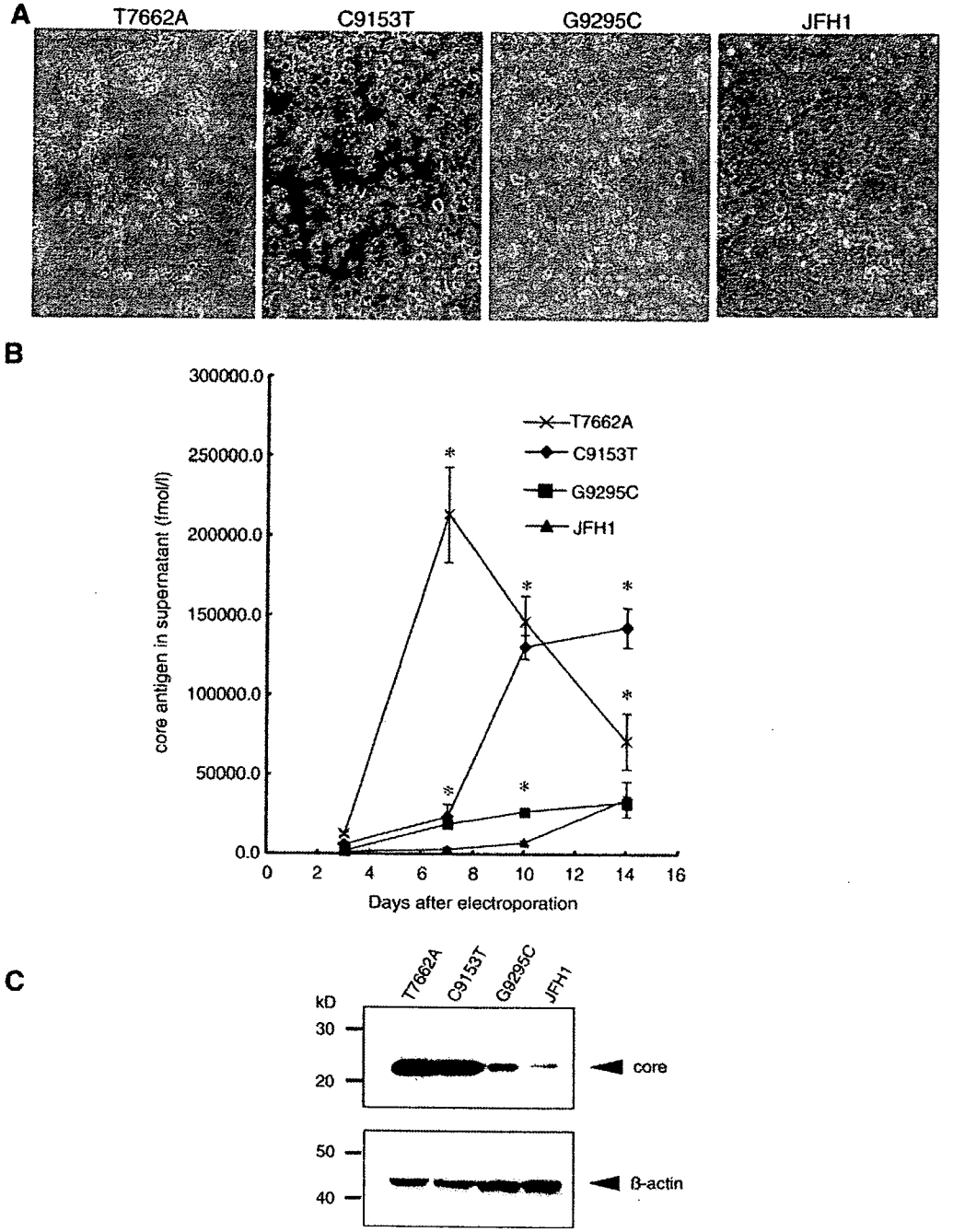

Fig. 9. Introduction of various mutations into the NS5B region of JFH1. The mutations identified in the cytopathic plaque P1#1; T7662A, C9153T, and G9295C were introduced individually into the parental JFH1. Each JFH1 mutant, T7662A, C9153T, and G9295C, RNA was transfected into Huh-7.5.1 cells by electroporation. The transfected cells were split every 3 to 5 days (see Materials and methods). (A) JFH1 mutants transfected Huh-7.5.1 cells were observed by phase-contrast microscopy at day 7 after transfection. (B) Levels of core antigen in the culture supernatants. The culture supernatants of transfected cells were collected on the days indicated, and the levels of core antigen were measured. Asterisks indicate p-values of less than 0.05. (C) The supernatants of JFH1 mutants transfected Huh-7.5.1 cells were transferred onto uninfected Huh-7.5.1 cells. The cells were harvested at 7 days after infection. Western blotting was performed using anti-core and anti-beta-actin.

thumb domain or affect the quaternary structure of the whole HCV replicase complex by altering surface affinity to other nonstructural proteins. Mapping of the amino acid substitutions in the RdRp tertiary structure has shown that the amino acid 2438 was located on the finger domain, and three amino acids, 2934, 2960, and 2985, were located on the outer surface of the thumb domain, which corresponds to the opposite side of the nucleotide tunnel. The other substitutions, 3000 and 3001, were within the domain of the polypeptide linking the polymerase to the membrane anchor (Lesburg et al., 1999). Very

recently, Zhong et al. have reported that long-term culture of HCV-JFH1 of more than 60 days leads to the evolution of certain mutations in the viral genome (Zhong et al., 2006). They identified amino acid changes in Core, E2, NS3, and NS5A regions, and especially E2 mutation increased infectivity and density changes of viruses. In our present study, however, we could not find those mutations in the virus subclones that we have isolated in the plaque assay technique. The discrepancy might be attributable to the presence or absence of HCV-CPE-induced cell clonal alteration of the host Huh-7.5.1 that occurs concomitantly with viral genetic evolution during long-term cell culture. Further analyses may be necessary to determine the most critical regions that regulate the viral replication efficiency and cytopathogenicity.

Interestingly, the mutant virus clones, T7662A (C2438S), C9153T (P2934S), and G9295C (R2985P), showed considerably higher replication efficiency and cytopathogenicity than the wild type JFH1 clone (Fig. 9). These results strongly suggest that certain NS5B mutations in the plaque-purified strains display more replication-efficient and cytopathic phenotypes. The present data are still preliminary. Further studies may be necessary to fully characterize these mutations and their functions, which include introduction of mutations of the HCV region and of the other plaque-purified viruses and combination of the mutations, and to study their effects on virus protein functions. We are at present analyzing derivative JFH1 clones in which other amino acid mutations were introduced.

Several clinical findings have suggested that HCV is not cytopathic and that antiviral immune responses such as cytotoxic T lymphocytes play important roles in HCV pathogenesis (Cerny and Chisari, 1999). On the other hand, apoptotic cell death is the first cellular response to many hepatotoxic events and has been implicated in the pathogenesis of liver diseases, such as viral hepatitis, autoimmune diseases, alcohol-induced injury, cholestasis, hepatocellular carcinoma, and fulminant hepatic failure (Canbay et al., 2004; Ghavami et al., 2005; Patel and Gores, 1995; Rodrigues et al., 2000; Rust and Gores, 2000; Thompson, 1995). Several clinical studies have shown that fulminant hepatic failure (FHF), from which HCV-JFH1 strain was isolated, showed far more hepatocyte apoptosis, as characterized by caspase activation and Fas-FasL expression, than chronic hepatitis and normal populations (Leifeld et al., 2006; Mita et al., 2005; Ryo et al., 2000). The ER stress markers GRP78 and ATF6 are upregulated in the HCV liver tissue as the histological grade advanced. In addition, GRP78 and ATF6 are upregulated as the histological grade increased in hepatocellular carcinoma (HCC) (Shuda et al., 2003) and proteomic analysis of HCC tissue samples has shown significant upregulation of HSP70 and GRP78 (Chuma et al., 2003; Takashima et al., 2003), indicating that these proteins may play important roles in HCV-induced hepatocarcinogenesis.

In conclusion, the cytopathic mutants of HCV-JFH1 strain were isolated by using plaque assay techniques. A mechanism of the cytopathic effects involved ER stress-mediated apoptosis that was triggered by virus infection. That process of cytopathic effects might explain one aspect of HCV-induced liver injury during acute infection. Further analyses of cellular effects on HCV replication may elucidate the pathogenesis of HCV infection and may define novel host factors as targets of antiviral chemotherapeutics.

Materials and methods

Reagents

Recombinant human interferon alpha-2b was from Schering-Plough (Kenilworth, NJ). Beta-mercaptoethanol was from Wako (Osaka, Japan). Anti-CD81 antibody (JS-81) was from BD Biosciences (Franklin Lakes, NJ) (Morikawa et al., 2007).

Cells and cell culture

Huh-7.5.1 cells (Zhong et al., 2005) (kindly provided by Dr Francis V. Chisari) were maintained in Dulbecco's modified minimal essential medium (DMEM, Sigma) supplemented with 2 mmol/l L-glutamine and 10% fetal bovine serum at 37 °C under 5.0% CO_2.

In vitro RNA synthesis and transfection

A plasmid, pJFH1-full (Wakita et al., 2005), which encodes the full-length HCV-JFH1 sequence, and two control plasmids for pJFH1-full were used; pJFH1/GND that is a replication incompetent mutant with a mutation in the NS5B GDD motif and pJFH1/ΔE1-E2 in which a coding region of the HCV envelope proteins was deleted. The HCV RNA was synthesized using the RiboMax Large Scale RNA Production System (Promega, Madison, WI), with the linearized pJFH1 plasmid as template. After DNaseI (RQ-1 RNase-free DNase, Promega) treatment, the transcribed HCV-RNA was purified using ISOGEN (Nippon Gene, Tokyo, Japan). For the RNA transfection, Huh-7.5.1 cells were washed twice, and 5×10^6 cells were resuspended in Opti-MEM I (Invitrogen, Carlsbad, CA) containing 10 μg of HCV RNA, transferred into a 4-mm electroporation cuvette, and subjected to an electric pulse (1050 μF and 270 V) using the Easy Ject system (EquiBio, Mieddlesex, UK). After electroporation, the cell suspension was left for 5 min at room temperature and then incubated under normal culture conditions in a 10-cm diameter cell culture dish. The transfected cells were split every 3 to 5 days. The culture supernatants were subsequently transferred onto uninfected Huh-7.5.1 cells. The levels of HCV replication and viral protein expression were detected by real-time PCR, western blotting, and immunocytochemistry.

HCV subgenomic replicon constructs

HCV subgenomic replicon plasmid pRep-Feo was derived from the HCV-N strain pHCV1bneo-delS (Tanabe et al., 2004) and pSGR-JFH1 was from the HCV-JFH1 strain (Kato et al., 2003). The replicon RNA was synthesized from pRep-Feo or pSGR-JFH1 and transfected into Huh-7.5.1 cells. After culture in the presence of G418 (Wako), cell lines stably expressing the replicon were established.

Real-time RT-PCR analysis

Total cellular RNA was isolated using ISOGEN (Nippon Gene). Two micrograms of total cellular RNA was used to generate cDNA from each sample using SuperScript II (Invitrogen) reverse transcriptase. Expression of mRNA was quantified using Quanti Tect SYBR Green PCR Master Mix (QIAGEN, Valencia, CA) and the ABI 7500 Real-Time PCR System (Applied Biosystems, Foster City, CA). The primers used were as follows: HCV-JFH1 sense (positions 7090 to 7109; 5′-TCA GAC AGA GCC TGA GTC CA-3′), HCV-JFH1 antisense (positions 7404 to 7423; 5′-AGT TGC TGG AGG GCT TCT GA-3′), beta-actin sense (5′-ACA ATG AAG ATC AAG ATC ATT GCT CCT CCT-3′), and beta-actin antisense (5′-TTT GCG GTG GAC GAT GGA GGG GCC GGA CTC-3′).

Quantification of HCV core antigen in the culture supernatant

The culture supernatants of JFH1-RNA transfected Huh-7.5.1 cells were collected on the days indicated, passed through a 0.45 μm filter (MILLEX-HA, Millipore, Bedford, MA), and stored at −80 °C. The levels of core antigen in the culture supernatants were measured using a chemiluminescence enzyme immunoassay (CLEIA) according to the manufacturer's protocol (Lumipulse Ortho HCV Antigen, Ortho-Clinical Diagnostics, Tokyo, Japan).

Western blotting

Western blotting was carried out as described previously (Tanabe et al., 2004; Yokota et al., 2003). Briefly, 10 μg of total cell lysate was separated by SDS–PAGE and blotted onto a polyvinylidene fluoride (PVDF) western blotting membrane. The membrane was incubated with the primary antibodies followed by a peroxidase-labeled anti-IgG antibody and visualized by chemiluminescence using the ECL western blotting Analysis System (Amersham Biosciences, Buckinghamshire, UK). The antibodies used were anti-core mouse monoclonal antibody 2H9 (provided by Dr. Wakita), anti-GRP78 goat monoclonal antibody, anti-GADD153/CHOP rabbit polyclonal antibody (Santa Cruz Biotechnology, Santa Cruz, CA), anti-eIF2-alpha, anti-phospho-eIF2-alpha rabbit polyclonal antibody (Cell Signaling, Danvers, CA), and anti-beta-actin antibody (Sigma).

Immunocytochemistry

HCV-JFH1-transfected or infected Huh-7.5.1 cells were cultured in Lab-Tek® Chamber Slide™ (Nalge Nunc International, Rochester, NY) or on 22-mm-round micro cover glasses (Matsunami, Tokyo, Japan). For detection of HCV-core and GRP78, cells were fixed with cold acetone for 15 min. The cells were incubated with the primary antibodies for 1 h at 37 °C and with Alexa Fluor 488 goat anti-mouse IgG antibody or Alexa Fluor 568 donkey anti-goat IgG antibody (Molecular Probes, Eugene, OR) for 1 h at room temperature. To analyze apoptosis of HCV-JFH1 infected cells, double staining for annexin V-FITC binding and for cellular DNA using propidium iodide (PI) was performed using an annexin V-Fluorescein Staining Kit (Wako, Osaka, Japan). Cells were visualized by a fluorescence microscopy (BZ-8000, KEYENCE, Osaka, Japan).

Plaque assay

Huh-7.5.1 cells were seeded in collagen-coated 60-mm-diameter plates at a density of $2–4 \times 10^5$ cells per plates and were incubated at 37 °C under 5.0% CO_2 (as described above). After overnight incubation, HCV-infected culture supernatants were serially diluted in a final volume of 2 ml per plates and transferred onto the cell monolayers. After ~5 h of incubation, the inocula were removed, and the cell monolayers were overlaid with 8 ml of culture medium (DMEM, 2 mmol/l L-glutamine and 10% fetal bovine serum) that contained 0.8% methylcellulose. After 7 to 12 days of incubation under normal culture conditions, formation of cytopathic plaque was visualized by staining the cell monolayers with 0.08% crystal violet solution (Sigma). The levels of cytotoxicity were evaluated by counting the plaques and calculating the titer (PFU/ml). Similarly, the titers of infectivity were evaluated by performing immunocytochemistry to detect foci of HCV-core-positive cells and calculating the infectious focus-forming units (FFU/ml).

Sequence analyses

The cDNA from the isolated JFH1 plaque was amplified from cytopathic virus-infected Huh-7.5.1 cells by RT-PCR and subjected to direct sequence determination. Nucleotide sequences were read from both strands using Big Dye Terminator Cycle Sequencing Ready Reaction kits (Applied Biosystems) and an automated DNA sequencer (ABI PRISM® 310 Genetic Analyzer; Applied Biosystems).

Establishment of mutant JFH1 clones

In order to introduce various mutations into the NS5B region of JFH1, plasmid pJFH1 was digested with *Hin*dIII and the DNA fragment encompassing nt. 8231 to 9731 was subcloned into the pBluescriptII SK+ phagemid vector (Stratagene, La Jolla, CA). The following mutations were introduced into the DNA fragment in the subcloning vector by site-directed mutagenesis (Quick-ChangeII Site-Directed Mutagenesis Kit; Stratagene): C9153T and G9295C, respectively. Finally, these *Hin*dIII–*Hin*dIII fragments were subcloned back into the parental plasmid pJFH1. The mutation T7662A-introduced PCR fragment (nt. 7421–7839) was subcloned into the T-Vector (pGEM-T Easy Vector Systems; Promega) and digested with *Rsr*II and *Bsr*GI. Finally, these *Rsr*II–*Bsr*GI fragments were subcloned back into the parental plasmid.

Statistical analyses

Statistical analyses were performed using the Student's *t*-test, and *p*-values of less than 0.05 were considered as statistically significant.

Acknowledgments

We are indebted to Dr. Francis V. Chisari for providing the Huh-7.5.1 cell line. This study was supported by grants from the Japan Society for the Promotion of Science, Miyakawa Memorial Research Foundation, and Viral Hepatitis Research Foundation of Japan.

References

Bartenschlager, R., Lohmann, V., 2000. Replication of hepatitis C virus. J. Gen. Virol. 81 (Pt 7), 1631–1648.

Benali-Furet, N.L., Chami, M., Houel, L., De Giorgi, F., Vernejoul, F., Lagorce, D., Buscail, L., Bartenschlager, R., Ichas, F., Rizzuto, R., Paterlini-Brechot, P., 2005. Hepatitis C virus core triggers apoptosis in liver cells by inducing ER stress and ER calcium depletion. Oncogene 24 (31), 4921–4933.

Blight, K.J., Kolykhalov, A.A., Rice, C.M., 2000. Efficient initiation of HCV RNA replication in cell culture. Science 290 (5498), 1972–1974.

Blight, K.J., McKeating, J.A., Rice, C.M., 2002. Highly permissive cell lines for subgenomic and genomic hepatitis C virus RNA replication. J. Virol. 76 (24), 13001–13014.

Borisevich, V., Seregin, A., Nistler, R., Mutabazi, D., Yamshchikov, V., 2006. Biological properties of chimeric West Nile viruses. Virology 349 (2), 371–381.

Canbay, A., Friedman, S., Gores, G.J., 2004. Apoptosis: the nexus of liver injury and fibrosis. Hepatology 39 (2), 273–278.

Cerny, A., Chisari, F.V., 1999. Pathogenesis of chronic hepatitis C: immunological features of hepatic injury and viral persistence. Hepatology 30 (3), 595–601.

Choukhi, A., Ung, S., Wychowski, C., Dubuisson, J., 1998. Involvement of endoplasmic reticulum chaperones in the folding of hepatitis C virus glycoproteins. J. Virol. 72 (5), 3851–3858.

Chuma, M., Sakamoto, M., Yamazaki, K., Ohta, T., Ohki, M., Asaka, M., Hirohashi, S., 2003. Expression profiling in multistage hepatocarcinogenesis: identification of HSP70 as a molecular marker of early hepatocellular carcinoma. Hepatology 37 (1), 198–207.

Despres, P., Frenkiel, M.P., Deubel, V., 1993. Differences between cell membrane fusion activities of two dengue type-1 isolates reflect modifications of viral structure. Virology 196 (1), 209–219.

Despres, P., Flamand, M., Ceccaldi, P.E., Deubel, V., 1996. Human isolates of dengue type 1 virus induce apoptosis in mouse neuroblastoma cells. J. Virol. 70 (6), 4090–4096.

Ferri, K.F., Kroemer, G., 2001. Organelle-specific initiation of cell death pathways. Nat. Cell Biol. 3 (11), E255–E263.

Ghavami, S., Hashemi, M., Kadkhoda, K., Alavian, S.M., Bay, G.H., Los, M., 2005. Apoptosis in liver diseases—detection and therapeutic applications. Med. Sci. Monit. 11 (11), RA337–RA345.

Gosert, R., Egger, D., Lohmann, V., Bartenschlager, R., Blum, H.E., Bienz, K., Moradpour, D., 2003. Identification of the hepatitis C virus RNA replication complex in Huh-7 cells harboring subgenomic replicons. J. Virol. 77 (9), 5487–5492.

Harding, H.P., Zhang, Y., Ron, D., 1999. Protein translation and folding are coupled by an endoplasmic-reticulum-resident kinase. Nature 397 (6716), 271–274.

He, B., 2006. Viruses, endoplasmic reticulum stress, and interferon responses. Cell Death Differ. 13 (3), 393–403.

Hinshaw, V.S., Olsen, C.W., Dybdahl-Sissoko, N., Evans, D., 1994. Apoptosis: a mechanism of cell killing by influenza A and B viruses. J. Virol. 68 (6), 3667–3673.

Jordan, R., Wang, L., Graczyk, T.M., Block, T.M., Romano, P.R., 2002. Replication of a cytopathic strain of bovine viral diarrhea virus activates PERK and induces endoplasmic reticulum stress-mediated apoptosis of MDBK cells. J. Virol. 76 (19), 9588–9599.

Kato, T., Furusaka, A., Miyamoto, M., Date, T., Yasui, K., Hiramoto, J., Nagayama, K., Tanaka, T., Wakita, T., 2001. Sequence analysis of hepatitis C virus isolated from a fulminant hepatitis patient. J. Med. Virol. 64 (3), 334–339.

Kato, T., Date, T., Miyamoto, M., Furusaka, A., Tokushige, K., Mizokami, M., Wakita, T., 2003. Efficient replication of the genotype 2a hepatitis C virus subgenomic replicon. Gastroenterology 125 (6), 1808–1817.

Kato, N., Nakamura, T., Dansako, H., Namba, K., Abe, K., Nozaki, A., Naka, K., Ikeda, M., Shimotohno, K., 2005. Genetic variation and dynamics of hepatitis C virus replicons in long-term cell culture. J. Gen. Virol. 86 (Pt 3), 645–656.

Kaufman, R.J., 1999. Stress signaling from the lumen of the endoplasmic reticulum: coordination of gene transcriptional and translational controls. Genes Dev. 13 (10), 1211–1233.

Koutsoudakis, G., Herrmann, E., Kallis, S., Bartenschlager, R., Pietschmann, T., 2007. The level of CD81 cell surface expression is a key determinant for productive entry of hepatitis C virus into host cells. J. Virol. 81 (2), 588–598.

Kummerer, B.M., Meyers, G., 2000. Correlation between point mutations in NS2 and the viability and cytopathogenicity of Bovine viral diarrhea virus strain Oregon analyzed with an infectious cDNA clone. J. Virol. 74 (1), 390–400.

Leifeld, L., Nattermann, J., Fielenbach, M., Schmitz, V., Sauerbruch, T., Spengler, U., 2006. Intrahepatic activation of caspases in human fulminant hepatic failure. Liver Int. 26 (7), 872–879.

Lesburg, C.A., Cable, M.B., Ferrari, E., Hong, Z., Mannarino, A.F., Weber, P.C., 1999. Crystal structure of the RNA-dependent RNA polymerase from hepatitis C virus reveals a fully encircled active site. Nat. Struct. Biol. 6 (10), 937–943.

Liberman, E., Fong, Y.L., Selby, M.J., Choo, Q.L., Cousens, L., Houghton, M., Yen, T.S., 1999. Activation of the grp78 and grp94 promoters by hepatitis C virus E2 envelope protein. J. Virol. 73 (5), 3718–3722.

Lindenbach, B.D., Evans, M.J., Syder, A.J., Wolk, B., Tellinghuisen, T.L., Liu, C.C., Maruyama, T., Hynes, R.O., Burton, D.R., McKeating, J.A., Rice, C.M., 2005. Complete replication of hepatitis C virus in cell culture. Science 309 (5734), 623–626.

Lohmann, V., Korner, F., Koch, J., Herian, U., Theilmann, L., Bartenschlager, R., 1999. Replication of subgenomic hepatitis C virus RNAs in a hepatoma cell line. Science 285 (5424), 110–113.

Maekawa, S., Enomoto, N., Sakamoto, N., Kurosaki, M., Ueda, E., Kohashi, T., Watanabe, H., Chen, C.H., Yamashiro, T., Tanabe, Y., Kanazawa, N., Nakagawa, M., Sato, C., Watanabe, M., 2004. Introduction of NS5A mutations enables subgenomic HCV replicon derived from chimpanzee-infectious HC-J4 isolate to replicate efficiently in Huh-7 cells. J. Viral Hepatitis 11 (5), 394–403.

Mendez, E., Ruggli, N., Collett, M.S., Rice, C.M., 1998. Infectious bovine viral diarrhea virus (strain NADL) RNA from stable cDNA clones: a cellular insert determines NS3 production and viral cytopathogenicity. J. Virol. 72 (6), 4737–4745.

Meyers, G., Thiel, H.J., 1996. Molecular characterization of pestiviruses. Adv. Virus Res. 47, 53–118.

Mita, A., Hashikura, Y., Tagawa, Y., Nakayama, J., Kawakubo, M., Miyagawa, S., 2005. Expression of Fas ligand by hepatic macrophages in patients with fulminant hepatic failure. Am. J. Gastroenterol. 100 (11), 2551–2559.

Mori, K., 2000. Tripartite management of unfolded proteins in the endoplasmic reticulum. Cell 101 (5), 451–454.

Morikawa, K., Zhao, Z., Date, T., Miyamoto, M., Murayama, A., Akazawa, D., Tanabe, J., Sone, S., Wakita, T., 2007. The roles of CD81 and glycosaminoglycans in the adsorption and uptake of infectious HCV particles. J. Med. Virol. 79 (6), 714–723.

Mottola, G., Cardinali, G., Ceccacci, A., Trozzi, C., Bartholomew, L., Torrisi, M.R., Pedrazzini, E., Bonatti, S., Migliaccio, G., 2002. Hepatitis C virus nonstructural proteins are localized in a modified endoplasmic reticulum of cells expressing viral subgenomic replicons. Virology 293 (1), 31–43.

Munro, S., Pelham, H.R., 1986. An Hsp70-like protein in the ER: identity with the 78 kD glucose-regulated protein and immunoglobulin heavy chain binding protein. Cell 46 (2), 291–300.

Nakagawa, M., Sakamoto, N., Tanabe, Y., Koyama, T., Itsui, Y., Takeda, Y., Chen, C.H., Kakinuma, S., Oooka, S., Maekawa, S., Enomoto, N., Watanabe, M., 2005. Suppression of hepatitis C virus replication by cyclosporin a is mediated by blockade of cyclophilins. Gastroenterology 129 (3), 1031–1041.

Pahl, H.L., 1999. Signal transduction from the endoplasmic reticulum to the cell nucleus. Physiol. Rev. 79 (3), 683–701.

Patel, T., Gores, G.J., 1995. Apoptosis and hepatobiliary disease. Hepatology 21 (6), 1725–1741.

Pavio, N., Romano, P.R., Graczyk, T.M., Feinstone, S.M., Taylor, D.R., 2003. Protein synthesis and endoplasmic reticulum stress can be modulated by the hepatitis C virus envelope protein E2 through the eukaryotic initiation factor 2alpha kinase PERK. J. Virol. 77 (6), 3578–3585.

Quaresma, J.A., Barros, V.L., Pagliari, C., Fernandes, E.R., Guedes, F., Takakura, C.F., Andrade Jr., H.F., Vasconcelos, P.F., Duarte, M.I., 2006. Revisiting the liver in human yellow fever: virus-induced apoptosis in hepatocytes associated with TGF-beta, TNF-alpha and NK cells activity. Virology 345 (1), 22–30.

Rodrigues, C.M., Brites, D., Serejo, F., Costa, A., Ramalho, F., De Moura, M.C., 2000. Apoptotic cell death does not parallel other indicators of liver damage in chronic hepatitis C patients. J. Viral Hepatitis 7 (3), 175–183.

Rust, C., Gores, G.J., 2000. Apoptosis and liver disease. Am. J. Med. 108 (7), 567–574.

Ryo, K., Kamogawa, Y., Ikeda, I., Yamauchi, K., Yonehara, S., Nagata, S., Hayashi, N., 2000. Significance of Fas antigen-mediated apoptosis in human fulminant hepatic failure. Am. J. Gastroenterol. 95 (8), 2047–2055.

Sato, H., Takimoto, T., Tanaka, S., Ogura, H., Shiraishi, K., Tanaka, J., 1989. Cytopathic effects induced by Epstein–Barr virus replication in epithelial nasopharyngeal carcinoma hybrid cells. J. Virol. 63 (8), 3555–3559.

Shinoura, N., Yoshida, Y., Tsunoda, R., Ohashi, M., Zhang, W., Asai, A., Kirino, T., Hamada, H., 1999. Highly augmented cytopathic effect of a fiber-mutant E1B-defective adenovirus for gene therapy of gliomas. Cancer Res. 59 (14), 3411–3416.

Shuda, M., Kondoh, N., Imazeki, N., Tanaka, K., Okada, T., Mori, K., Hada, A., Arai, M., Wakatsuki, T., Matsubara, O., Yamamoto, N., Yamamoto, M., 2003. Activation of the ATF6, XBP1 and grp78 genes in human hepatocellular carcinoma: a possible involvement of the ER stress pathway in hepatocarcinogenesis. J. Hepatol. 38 (5), 605–614.

Su, H.L., Liao, C.L., Lin, Y.L., 2002. Japanese encephalitis virus infection initiates endoplasmic reticulum stress and an unfolded protein response. J. Virol. 76 (9), 4162–4171.

Sumpter Jr., R., Loo, Y.M., Foy, E., Li, K., Yoneyama, M., Fujita, T., Lemon, S.M., Gale Jr., M., 2005. Regulating intracellular antiviral defense and permissiveness to hepatitis C virus RNA replication through a cellular RNA helicase, RIG-I. J. Virol. 79 (5), 2689–2699.

Takashima, M., Kuranitsu, Y., Yokoyama, Y., Iizuka, N., Toda, T., Sakaida, I., Okita, K., Oka, M., Nakamura, K., 2003. Proteomic profiling of heat shock protein 70 family members as biomarkers for hepatitis C virus-related hepatocellular carcinoma. Proteomics 3 (12), 2487–2493.

Tanabe, Y., Sakamoto, N., Enomoto, N., Kurosaki, M., Ueda, E., Maekawa, S., Yamashiro, T., Nakagawa, M., Chen, C.H., Kanazawa, N., Kakinuma, S., Watanabe, M., 2004. Synergistic inhibition of intracellular hepatitis C virus replication by combination of ribavirin and interferon-alpha. J. Infect. Dis. 189 (7), 1129–1139.

Tardif, K.D., Mori, K., Siddiqui, A., 2002. Hepatitis C virus subgenomic replicons induce endoplasmic reticulum stress activating an intracellular signaling pathway. J. Virol. 76 (15), 7453–7459.

Tardif, K.D., Mori, K., Kaufman, R.J., Siddiqui, A., 2004. Hepatitis C virus suppresses the IRE1-XBP1 pathway of the unfolded protein response. J. Biol. Chem. 279 (17), 17158–17164.

Thompson, C.B., 1995. Apoptosis in the pathogenesis and treatment of disease. Science 267 (5203), 1456–1462.

Vaughn, D.W., Hoke Jr., C.H., 1992. The epidemiology of Japanese encephalitis: prospects for prevention. Epidemiol. Rev. 14, 197–221.

Wakita, T., Pietschmann, T., Kato, T., Date, T., Miyamoto, M., Zhao, Z., Murthy, K., Habermann, A., Krausslich, H.G., Mizokami, M., Bartenschlager, R., Liang, T.J., 2005. Production of infectious hepatitis C virus in tissue culture from a cloned viral genome. Nat. Med. 11 (7), 791–796.

Waxman, L., Whitney, M., Pollok, B.A., Kuo, L.C., Darke, P.L., 2001. Host cell factor requirement for hepatitis C virus enzyme maturation. Proc. Natl. Acad. Sci. U. S. A. 98 (24), 13931–13935.

Yanagiya, A., Jia, Q., Ohka, S., Horie, H., Nomoto, A., 2005. Blockade of the poliovirus-induced cytopathic effect in neural cells by monoclonal antibody against poliovirus or the human poliovirus receptor. J. Virol. 79 (3), 1523–1532.

Yi, M., Ma, Y., Yates, J., Lemon, S.M., 2007. Compensatory mutations in E1, p7, NS2, and NS3 enhance yields of cell culture-infectious intergenotypic chimeric hepatitis C virus. J. Virol. 81 (2), 629–638.

Yokota, T., Sakamoto, N., Enomoto, N., Tanabe, Y., Miyagishi, M., Maekawa, S., Yi, L., Kurosaki, M., Taira, K., Watanabe, M., Mizusawa, H., 2003. Inhibition of intracellular hepatitis C virus replication by synthetic and vector-derived small interfering RNAs. EMBO Rep. 4 (6), 602–608.

Yu, C.Y., Hsu, Y.W., Liao, C.L., Lin, Y.L., 2006. Flavivirus infection activates the XBP1 pathway of the unfolded protein response to cope with endoplasmic reticulum stress. J. Virol. 80 (23), 11868–118680.

Zheng, Y., Gao, B., Ye, L., Kong, L., Jing, W., Yang, X., Wu, Z., Ye, L., 2005. Hepatitis C virus non-structural protein NS4B can modulate an unfolded protein response. J. Microbiol. 43 (6), 529–536.

Zhong, J., Gastaminza, P., Cheng, G., Kapadia, S., Kato, T., Burton, D.R., Wieland, S.F., Uprichard, S.L., Wakita, T., Chisari, F.V., 2005. Robust hepatitis C virus infection in vitro. Proc. Natl. Acad. Sci. U. S. A. 102 (26), 9294–9299.

Zhong, J., Gastaminza, P., Chung, J., Stamataki, Z., Isogawa, M., Cheng, G., McKeating, J.A., Chisari, F.V., 2006. Persistent hepatitis C virus infection in vitro: coevolution of virus and host. J. Virol. 80 (22), 11082–11093.

GASTROENTEROLOGY 2007;132:311–320

A Cell-Based, High-Throughput Screen for Small Molecule Regulators of Hepatitis C Virus Replication

SUN SUK KIM,[*,‡] LEE F. PENG,[*,§,‖] WENYU LIN,[*] WON-HYEOK CHOE,[*] NAOYA SAKAMOTO,[¶] STUART L. SCHREIBER,[§,‖,#] and RAYMOND T. CHUNG[*]

[*]GI Unit, Department of Medicine, Massachusetts General Hospital, Boston Massachusetts; [‡]Department of Gastroenterology and Hepatology, Gachon University Gil Medical Center, Incheon, Korea; [§]Department of Chemistry and Chemical Biology, Harvard University, Cambridge, MA; [‖]The Broad Institute of Harvard and MIT, Cambridge, MA; [¶]Department of Gastroenterology and Hepatology, Tokyo Medical and Dental University, Tokyo, Japan; [#]Howard Hughes Medical Institute, Chevy Chase, Maryland

Background & Aims: **Only half of patients with chronic hepatitis C virus (HCV) infection experience sustained virologic response to pegylated-interferon and ribavirin, which cause numerous side effects. Thus, the identification of more effective and better tolerated agents is a high priority. We applied chemical biology to screen small molecules that regulate HCV.** ***Methods:*** **We first optimized the Huh7/Rep-Feo replicon cell line for the 384-well microplate format and used this line to screen a large library of well-characterized, known biologically active compounds using automated technology. After identifying several molecules capable of either stimulating or inhibiting HCV replication in this primary screen, we then validated our hit compounds using a full-length HCV replicon cell line in secondary screens.** ***Results:*** **We identified and validated a number of antiviral and proviral agents, including HMG-CoA reductase inhibitors (antiviral) and corticosteroids (proviral). The finding of increased replication associated with corticosteroids suggests that these agents directly promote viral replication independent of their suppressive effects on the immune response. The finding of antiviral activity associated with the HMG-CoA reductase inhibitors implies an important role for lipid metabolism in the viral life cycle.** ***Conclusions:*** **We have developed a simple, reproducible, and reliable cell-based high-throughput screening assay system using an HCV replicon model to identify small molecules that regulate HCV replication. This method can be used to identify not only putative antiviral agents, but also cellular regulators of viral replication.**

Hepatitis C virus (HCV) infects over 170 million people worldwide and frequently leads to cirrhosis, liver failure, and hepatocellular carcinoma.[1] The current best therapy for chronic hepatitis C is a combination of pegylated interferon (PEG-IFN) and ribavirin. Although the sustained virologic response (SVR) rate approaches 80% for patients with genotypes 2 and 3, the SVR rate is limited to about 45% for HCV genotype 1, which is responsible for about 75% of all cases of HCV in the United States.[2] Furthermore, interferon is parenteral, has an unfavorable side effect profile, and its use requires frequent monitoring for toxicity, ultimately causing 20% of patients to discontinue therapy.[2] The identification of more effective and better tolerated agents is therefore a high priority.

The advancement of our understanding of the mechanisms underlying HCV replication and persistence and the development of new antiviral therapeutics has been hampered by the lack of tractable model systems capable of robust viral replication.[3] However, the recent development of models capable of high-level autonomous HCV RNA replication has greatly facilitated the evaluation of antiviral activities of new anti-HCV drug candidates as well as the study of viral RNA replication and persistence.[4]

In parallel with advances in the cultivation of HCV, chemical biology has emerged as a powerful tool to study biological processes using small organic molecules.[5,6] In the field of chemical biology, 2 general screening approaches have been employed—reverse and forward chemical genetics.[6] Reverse chemical genetics, which has historically been used, starts with a given enzymatic or molecular target and attempts to identify small organic molecules capable of binding to it. The weakness of this approach is that not all binding interactions identified are capable of producing the desired biological effect. On the other hand, forward chemical genetics involves screening perturbagens, such as small molecules, for their effects on a given phenotypic endpoint. All hits, therefore, by definition are biologically meaningful in such a screen. In our case, we were interested in identifying perturbagens capable of modulating HCV replication. Because the level of HCV replication can now be assayed,

Abbreviations used in this paper: HCV, hepatitis C virus; HMG-CoA, hydroxyl-methyl-glutaryl coenzyme A; HTS, high-throughput screening; PDE, phosphodiesterase; PEG-IFN, pegylated interferon; S/B, signal-to-background; SVR, sustained virologic response.

0016-5085/07/$32.00
doi:10.1053/j.gastro.2006.10.032

use of the forward chemical genetics approach is now possible.

To efficiently determine whether small molecules exert a certain biological effect in a suitable assay system, rapid high-throughput screening (HTS) methods have been developed. Using the high-density 384-well plate format, it is possible to efficiently and successfully conduct high-throughput phenotypic screens on mammalian cell constructs bearing reporter genes, such as those found in HCV replicon systems, with large libraries of small molecules.[7]

Thus far, however, efficient HTS for HCV drug discovery has remained elusive. Although HCV replicon systems have been established as efficient cell-based screening platforms, no true HTS methods utilizing these systems have been described to date. Experimental barriers have included low signal-to-background ratio and the added burden of complex processing steps, such as washing, aspiration, and lysis prior to signal read-out.

The subgenomic Huh7/Rep-Feo HCV replicon cell line[8] appears to be particularly well suited to automated HTS methods, so it was selected for further assay development. This replicon was derived from a chimpanzee infectious clone (strain HCV-N, genotype 1b). In this replicon, the structural genes have been replaced by a reporter gene. The chimeric reporter gene Feo encodes the firefly luciferase protein fused in-frame with neomycin phosphotransferase. This Huh7/Rep-Feo cell supports high levels of autonomous HCV RNA replication because it was derived from the HCV-N strain, which carries an adaptive mutation in NS5A that confers high-level replication in tissue culture. Furthermore, the level of luciferase correlates well with levels of HCV RNA production, so that luciferase can be used as a reliable surrogate marker for HCV replication. The use of luciferase as a reporter permits quantitative and high-throughput detection of HCV replication levels. The specific use of firefly luciferase makes this replicon especially well-suited for automation, because the luciferase reagent can be added directly to the cell culture system prior to signal detection without the need for cell lysis, washing, or aspiration.

In the course of our attempts to apply chemical biology to the elucidation of the regulation of HCV replication, we first optimized the Huh7/Rep-Feo replicon for the 384-well microplate format and then used it to screen a library of known bioactive compounds using automated technology. After identifying several molecules capable of either stimulating or inhibiting HCV replication in this primary screen, we then validated our hit compounds in secondary screens. Here we describe a simple, reproducible, and reliable cell-based HTS assay system using a HCV replicon model to identify small molecules that regulate HCV replication and further characterize the antiviral properties of the HMG-CoA reductase inhibitors, as well as the proviral properties of corticosteroids.

Materials and Methods

HCV Replicon System–Primary Screening

Cells were propagated in Dulbecco's Modified Eagle's medium (DMEM) containing 10% fetal bovine serum (FBS) supplemented with 1% penicillin-streptomycin, and 500 μg of Geneticin (Invitrogen Corp., Carlsbad, CA) /mL. Cells were cultured in a 37°C, 5% CO_2-humidified incubator for all experiments. To decrease day-to-day variability in the assay, a large homogenous population of subconfluent cells was passaged so that a similar lot of cells could be used throughout the HTS assay.

Optimization of Huh-7/Rep-Feo Cells for the 384-Well Plate Format

The Huh7/Rep-Feo cells were first optimized for the 96-well plate format. Peginterferon-alfa-2b (PEG-Intron; Schering Corp., Kenilworth, NJ) was used as a positive control for inhibition. Cells were seeded at densities of 5000 and 10,000 cells/well in 100 μL of medium in 96-well plates. The cells were allowed to attach overnight (~24 hours) before addition of PEG-IFN at various concentrations (day 0). The plates were then incubated further, and measurements were taken at 24, 48, and 72 hours. At each time point, the plates were equilibrated at room temperature, an equal volume of Bright-Glo reagent (Promega, Madison, WI) was added, and the plates were read in a LumiCount (Packard BioScience Company, Downers Grove, IL) luminometer. For the 384-well plate format, cells were seeded at densities of 1000, 2500, and 5000 cells/well in 30 μL of medium. The remainder of the experiment was carried out as described for 96-well plates. Results were expressed as the mean of 3 replicate wells.

Primary Screening–HTS

Information about the library of known bioactive compounds that was screened and the general automated HTS protocol is available at http://www.broad.harvard.edu/chembio/index.html.

Based on the results of optimization experiments in the 384-well plate format, the general HTS protocol was adapted as follows. Unless otherwise indicated, cells were incubated at all times in a humidified environment with 5% CO_2 at 37°C. The assay was initiated by plating 30 μL of medium containing 2000 cells/well into white 384-well opaque-bottom plates (Nunc, Rochester, NY) using an automated plate filler (Bio-Tek μFiller; Winsooki, VT) and allowing the cells to adhere for 24 hours. One hundred nL of compound stock solutions in DMSO was transferred from stock plates into the 384-well assay plates using an automated pin-based compound transfer robot (CyBio CyBi-Well vario; Woburn, MA). The final compound concentration in each well was estimated to be approximately 10–50 μM, with most compounds at 33 μM. The wells

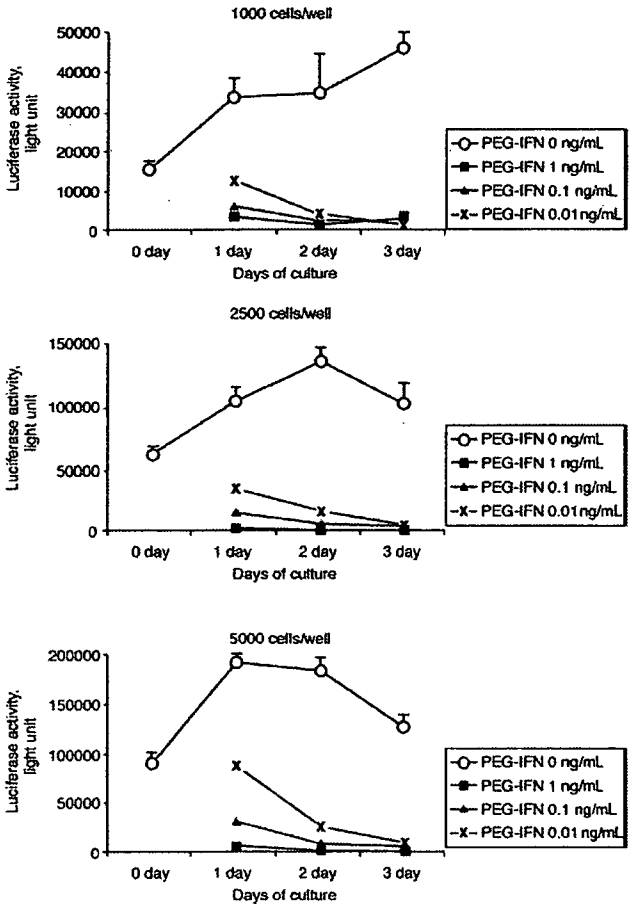

Figure 1. Luciferase activity of different cell inoculation concentrations in the 384-well plate format. Different concentrations of PEG-IFN were used as a positive control and to determine signal-to-background (S/B) ratio. HCV RNA replication levels were determined by luciferase activity, as described in Material and Methods. Each point represents the average of 3 data points, with the standard deviation represented as data bars.

contained 0.33% DMSO by volume. The cells were then incubated for another 48 hours. The luminescent signal from each plate was detected using an automated plate reader (Perkin-Elmer Envision 1; Wellesley, MA). This screen was performed in duplicate. For negative controls, entire DMSO-treated control plates were employed, in addition to DMSO-only control wells that were incorporated into each compound assay plate. The cells were assayed for luciferase activity using the Bright-Glo Luciferase assay system (Promega), following the manufacturer's instructions. As a counter-screen, cell viability was assessed using the CellTiterGlo Luminescent cell viability assay (Promega) following the manufacturer's instructions.

Computational Data Analysis–Primary Screening

For each replicate, a mock-treatment distribution based on the total population of mock (DMSO) controls in that replicate was built. Each compound was independently assigned a sign (ie, "+" or "−") Z-score. Z-scores are calculated by dividing each background-subtracted, compound-treated well by the global standard deviation. A global standard deviation of the background-subtracted, mock-treated wells is calculated over the entire experiment. This distribution was determined to be consistent with experimental noise observed under cell-based assay conditions. The resulting collection of continuous-valued Z-scores represents the primary data set to be used for further analysis. The composite Z-score was calculated as a vector projection of each Z-score in duplicate onto an imaginary line of perfect reproducibility. Reproducibility is the cosine of the angle between each Z-score and that imaginary line; it is dimensionless and ranges from −1 to +1. For analyses dependent upon discrete (ie, binned) outcome states, composite Z-score data were further subjected to a threshold that resulted in each measurement being scored as a high- or low-signal outlier, or as a nonoutlier, from the mock-treatment distribution, based on the possibility that the measurement could be explained by assay noise ($P_{noise} < .0005$).

The primary data were analyzed using the commercial software packages Pipeline Pilot (SciTegic, San Diego, CA) and SpotFire (SpotFire, Inc., Somerville, MA). The means of the negative, DMSO-only controls were considered the zero point. For the bioactives library, compounds were considered hits for inhibiting replication if they had a composite Z-score of <-5.14 in the reporter gene screen, a reproducibility of >0.9 or <-0.9 in that screen, and a composite Z-score of >-2.57 in the cell viability screen. Compounds were considered hits for promoting replication if they had a composite Z-score of >5.14 in the reporter gene screen, a reproducibility of >0.9 or <-0.9 in that screen, and a composite Z-score of <2.57 in the cell viability screen.

HCV Replicon System–Secondary Assays

For validation, OR6 cells stably harboring the full-length genotype 1 replicon, ORN/C-5B/KE[9] were used to examine compound activity in a more authentic viral polyprotein context. This replicon was derived from the 1B-2 strain (strain HCV-O, genotype 1b), in which the *Renilla* luciferase gene is introduced as a fusion protein with neomycin to facilitate the monitoring of HCV replication. This construct contains a tissue culture adaptive mutation in the NS3 region. Cells were cultured in an identical manner to the Huh7/Rep-Feo cells.

Secondary Assays–Hit Validation

Several hits from primary HTS, as well as functionally related compounds, were purchased from Sigma (St. Louis, MO), Calbiochem (San Diego, CA), and Microsource (Gaylordsville, CT). Proviral compounds included (1) corticosteroids—triamcinolone acetonide, prednisolone, dexamethasone, and methylprednisolone, (2) PPAR-gamma ligands—N-(9-fluorenylmethoxy-car-

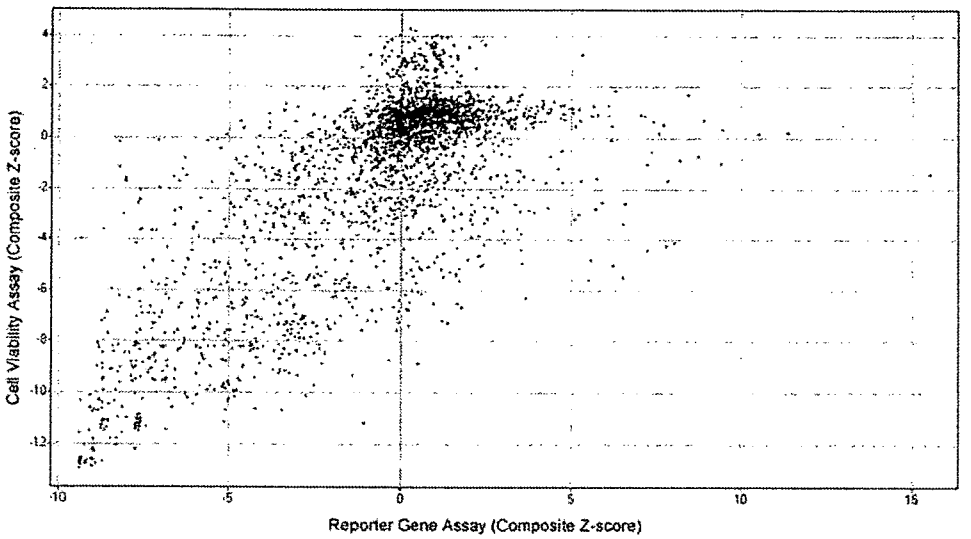

Figure 2. A graphical summary of the primary screening for the known bioactives library using Huh7/Rep-Feo cell. Each point represents 1 compound. The X-axis shows HCV replication as measured by normalized luciferase signal, expressed as the composite Z-score. The Y-axis shows cell viability as measured by normalized CellTiterGlo (Promega) signal, expressed as the composite Z-score.

bonyl)-L-leucine (Fmoc-Leu) and troglitazone, and (3) coumarins—marmesin, xanthyletin, dihydro-obliquin, warfarin, coumarin, citropen, and dicumarol. Antiviral compounds included (1) PDE inhibitors—MY-5445, trequinsin, zaprinast, and rolipram, (2) calcium channel blockers—tetrandrine, verapamil, nifedipine, diltiazem, and nimodipine, (3) MAPK inhibitors—SB-203580, SB-202190, and PD 98059, as well as a negative control (SB 202474), and (4) HMG-CoA reductase inhibitors—atorvastatin, simvastatin, mevastatin, lovastatin, fluvastatin, and pravastatin.

Ten mM of stock solutions of the individual compounds to be tested was prepared in the appropriate solvent (DMSO, ethanol, or H_2O, according to the manufacturer's information) and stored at −20°C.

Cells were seeded into 96-well plates at a density of 2000 cells/well in 100 μL of medium. The cells were incubated for 24 hours at 37°C to obtain the optimal level of adherence. Solutions of candidate hit compounds were added to wells to achieve final concentrations of 0.1, 1, 10, 50, and 100 μM. The final concentration of DMSO or ethanol in every well was 1% or less by volume. Mock solutions were used as a negative control. PEG-IFN and ribavirin were used as positive controls at various concentrations, alone and in combination. The plates were then incubated at 37°C with 5% CO_2 for 48 hours before they were analyzed. Luminescent signal was generated using the *Renilla* luciferase assay kit (Promega) according to the manufacturer's instructions. Signal was then detected using a LumiCount (Packard BioScience Company) luminometer. Cell viability was assessed using CellTiter-Glo (Promega), following the manufacturer's instructions. All experiments were performed in triplicate.

Secondary Assays–Data Analysis

Values were presented as a percentage of mock treated control, which was arbitrarily set at 100%. Data were expressed as the mean ± SD. Results were analyzed using a paired *t* test to determine the significance of observed differences between the values of control and individual concentrations and were considered significant if the *P* values were less than .05. Synergy calculations were performed using CalcuSyn (Biosoft; Cambridge, England).

Results

Optimization of Huh-7/Rep-Feo Cells for the 384-Well Plate Format

HCV replication in the subgenomic replicon cell model was tightly coupled to host cell growth conditions.[10,11] Experimentally, HCV RNA replication in the subgenomic replicon cell increased progressively over time, followed by a sharp decline when the cells reached 70% confluence. There was a good linear relationship between cell number and luciferase signal in test tube (data not shown). Inasmuch as the wells of microplates have a small culturable surface, the Huh7/Rep-Feo cells were optimized for both the 96-well and 384-well plate formats using PEG-IFN as a positive control. For 96-well plates, the signal-to-background (S/B) ratio was very high (over 100) when cells were incubated at a concentration of 5000 cells/well at culture day 0. The S/B ratio progressively increased over time, peaking at culture day 2 and then decreased from culture day 3 onward, when cells reached over 70% confluence. The antiviral activity of PEG-IFN progressively increased over time. On the other hand, although the initial S/B ratio at an inoculation

Table 1. Hits From the Primary HTS With the Known Bioactives Library

Compound name	R-CompZ	C-CompZ
Proviral hit compounds		
Diphenylurea	15.510	−1.415
Piceid	11.366	0.220
Iridin	10.529	0.162
Biochanin A diacetate	9.416	0.340
5,4′-dimethoxyflavone	9.391	−0.997
Chlorpropham	8.891	0.694
Tectorigenin	8.728	−0.737
N-(9-fluorenylmethoxycarbonyl)-L-leucine	8.440	1.676
7,4′-dimethoxyisoflavone	8.178	−0.852
Dihydro-obliquin	7.825	−1.676
Marmesin	7.700	0.502
Salicylanilide	7.562	0.169
Liquiritigenin dimethyl ether	7.417	0.654
Robustic acid	7.345	−0.546
3,7-dihydroxyflavone	7.226	−1.033
Methimazole	7.169	0.859
Colistimethate	7.040	0.885
Acacetin	6.278	1.846
6,4′-dimethoxyflavone	6.189	0.482
2-ethoxycarbonyl-2-hydroxy-5,7-dimethoxyisoflavanone	6.177	−0.085
Estrone	6.100	0.842
Fenspiride	6.088	1.234
Butirosin A	5.787	0.894
Xanthyletin	5.747	−1.589
Todralazine	5.653	1.222
Niflumic acid	5.297	−1.695
Triamcinolone	5.275	0.703
Cuneatin methyl ether	5.146	0.468
Antiviral hit compounds		
SB-203580	−8.244	−1.160
MY-5445	−8.237	−0.190
Swainsonine	−8.058	−1.577
Pifithrin	−8.043	−1.725
3-alpha-hydroxydeoxygedinin	−7.701	−2.563
(S)-propranolol	−7.629	−2.439
Andrographolide	−7.618	−2.064
Tetrandrine	−7.091	−0.134
Pregnenolone 16-alpha carbonitrile	−7.059	−1.994
Cyclopamine	−6.766	−2.005
Derrusnin	−6.642	−1.558
2,3,29-triacetoxy-24-nor-1,3,5,7-friedelatetraene	−6.474	−1.734
Atorvastatin	−6.385	−1.259
Coenzyme B-12	−6.300	−0.809
E-64-D	−6.252	−1.502
Deoxyandirobin lactone	−5.839	−2.412
3-beta-hydroxydeoxydesacetoxy-7-oxogedunin	−5.634	−0.128
U-37883A	−5.527	−1.749
Alachlor	−5.344	−0.075
Veratridine	−5.246	−0.415
1,2-alpha-epoxydeacetoxydihydrogedunin	−5.177	−2.414

R-CompZ, composite Z-score for reporter gene assay; C-CompZ, composite Z-score for cell viability assay.

concentration of 10,000 cells/well was higher than at 5000 cells/well, there was no significant increase of the S/B ratio over time (data not shown). For 384-well plates, the S/B ratio at an inoculation concentration of 1000 cells/well progressively increased over time, with a large standard deviation. The S/B ratio at an inoculation concentration of 5000 cells/well peaked at culture day 1, when an optimum level of confluence was reached. The S/B ratio at an inoculation concentration of 2500 cells/well was ideal, with the optimal S/B ratio achieved at culture day 2 (Figure 1). We therefore selected 2500 cells/well at culture day 2 for subsequent studies.

Primary Screening (HTS) Results

Figure 2 shows a graphical representation of the primary HTS results. Many compounds appeared to have strong antiviral activity when the luciferase reporter gene assay alone was considered. When these results were analyzed in conjunction with those of the cell viability assay, however, most of the potential antiviral hit compounds were cytotoxic and, therefore, false positives. For that reason, it is imperative to perform the primary HTS as a 2-dimensional assay with both the level of HCV replication and cell viability measurements, in order to minimize confounding from increased luciferase signals due to increased cell titer and decreased luciferase signals due to decreased cell titer.

Using the data analysis and hit selection criteria outlined in Materials and Methods, we identified 21 antiviral compounds that inhibited HCV replication and 28 proviral compounds that increased HCV replication (Table 1). The respective hit rates of 0.8% and 1.1% are consistent with hit rates for other biological screens performed using this library.

Proviral compounds included steroids (estrone, triamcinolone), coumarins (xanthylentin, dihydrobliquin, and marmesin), flavones, and a PPAR-gamma ligand (N- 9-fluorenylmethoxycarbonyl-L-leucine). Antiviral compounds included an HMG-CoA reductase inhibitor (atorvastatin), a beta-adrenergic blocker (propranolol), a calcium channel blocker (tetrandrine), a phosphodiesterase (PDE) inhibitor (MY-5445), and a p38 MAP kinase inhibitor (SB 203580). The finding of antiviral activity associated with the HMG-CoA reductase inhibitor was of particular interest, as the HMG-CoA reductase inhibitor lovastatin has recently been shown to exhibit anti-HCV activity.[12] Although corticosteroids have been assumed to increase HCV replication by means of host immunosuppression, they have not been reported to be a specific proviral agent for HCV independent of their general immunosuppressive activity.[13] SB-203580 has been previously reported to have mixed effects on HCV replication.[14,15]

Anti-HCV Activity of PEG-IFN and Ribavirin in the OR6 Replicon System

We tested PEG-IFN and ribavirin at various concentrations, alone and in combination, as it has been reported that OR6 cells bearing a genome-length HCV RNA replicon were sensitive to these agents.[9] The IC_{50} of

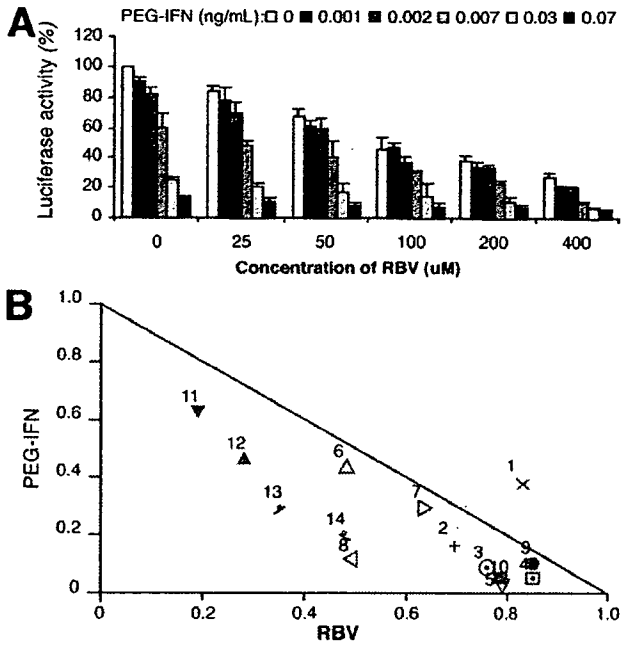

Figure 3. (*A*) Anti-HCV activity of PEG-IFN and ribavirin on HCV RNA replication in OR6 cell system. OR6 cells were cotreated with PEG-IFN (0, 0.001, 0.002, 0.007, 0.03, and 0.07 ng/mL) and ribavirin (0, 25, 50, 100, 200, and 400 μM) for 48 hours. Luciferase activity for HCV RNA replication levels is shown as a percentage of control. Each *bar* represents the average of triplicate data points with standard deviation represented as the *error bar*. (*B*) A normalized isobologram generated by CalcuSyn using the data from Figure 3*A*. *Points* below and to the left of the line represent synergy. Thirteen of the 14 concentration ratios examined demonstrate the synergistic effect of the combination of PEG-IFN and ribavirin.

PEG-IFN was between 0.007 and 0.03 ng/mL. The IC_{50} of ribavirin was between 50 μM and 100 μM (Figure 3*A*). As previously reported, the combination of ribavirin with PEG-IFN showed synergy (Figure 3*B*). These results demonstrate that HCV RNA replication in OR6 cells is highly sensitive to PEG-IFN, ribavirin, and a combination of both agents.

Hit Validation

Several proviral and antiviral hit compounds identified in the primary screen were selected for further validation on the basis of commercial availability and clinical interest. In order to examine compound activity in a more authentic viral polyprotein context, the validation assays were carried out using the OR6 full-length genotype 1b replicon. Multiple concentrations of each compound were used in order to generate an adequate dose-response curve. In addition to the actual hit compounds themselves, other compounds from the relevant compound classes were subjected to secondary validation assays.

Proviral compounds. Triamcinolone was confirmed to increase HCV replication in the full-length HCV replicon system (Figures 4*A* and *B*). Other corticosteroids (prednisolone, dexamethasone, and methylprednisolone) also increased HCV replication (Figures 4*A* and *B*). The PPAR gamma ligand, N- (9-fluorenylmethoxycarbonyl)-L-leucine, which was identified as a proviral hit in the primary screen, showed mild proviral activity. Troglitazone showed proviral activity at 1 and 10 μM. The decreased luciferase signal at 50 μM and above was due to cytotoxicity. Clofibrate, a PPAR alpha ligand, did not show a proviral effect. The coumarin compounds did not demonstrate any significant proviral activity (data not shown).

Antiviral compounds. Although the PDE inhibitor, MY5445, decreased the luciferase signal in a dose-related manner, it displayed significant cytotoxicity. Another PDE inhibitor in the bioactives library, trequinsin, was not identified as a hit in the primary screen, where it was tested at a concentration of 33 μM and found to be cytotoxic. It did, however, display antiviral activity at the lower concentrations of 1 and 10 μM in the validation assay, with significant cytotoxicity only at the higher concentrations of 50 and 100 μM (Figures 5*A* and *B*).

The p38 MAPK inhibitor, SB 203580, exhibited antiviral activity at a concentration of 10 μM and cytotoxicity at higher concentrations (Figures 5*C* and *D*). Other MAPK inhibitors, such as SB 202109, were inactive in both the primary screen and in the secondary assay (data not shown).

The antiviral effect of the calcium channel blocker, tetrandrine, could not be evaluated because of cytotoxicity in the secondary assay (Figures 5*E* and *F*). Other

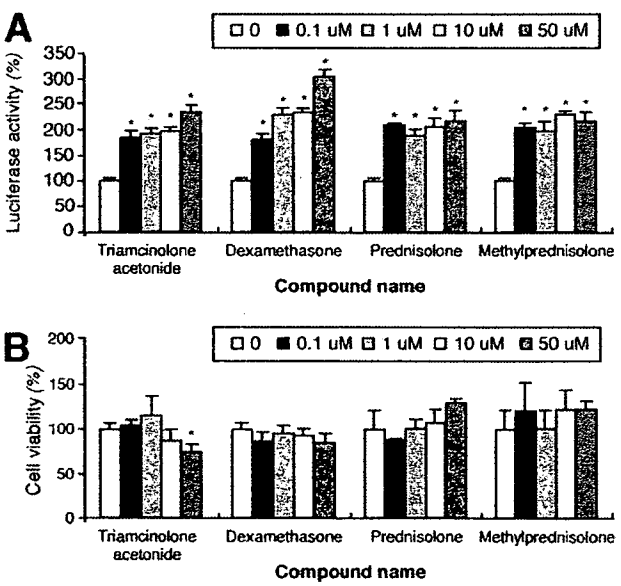

Figure 4. Results of secondary screening with corticosteroids. (*A*) Luciferase activity for HCV RNA replication levels is shown as a percentage of control. (*B*) Cell viability is also shown as a percentage of control. Each *bar* represents the average of triplicate data points with standard deviation represented as the *error bar*. *Denotes a significant difference from control of at least $P < .05$.

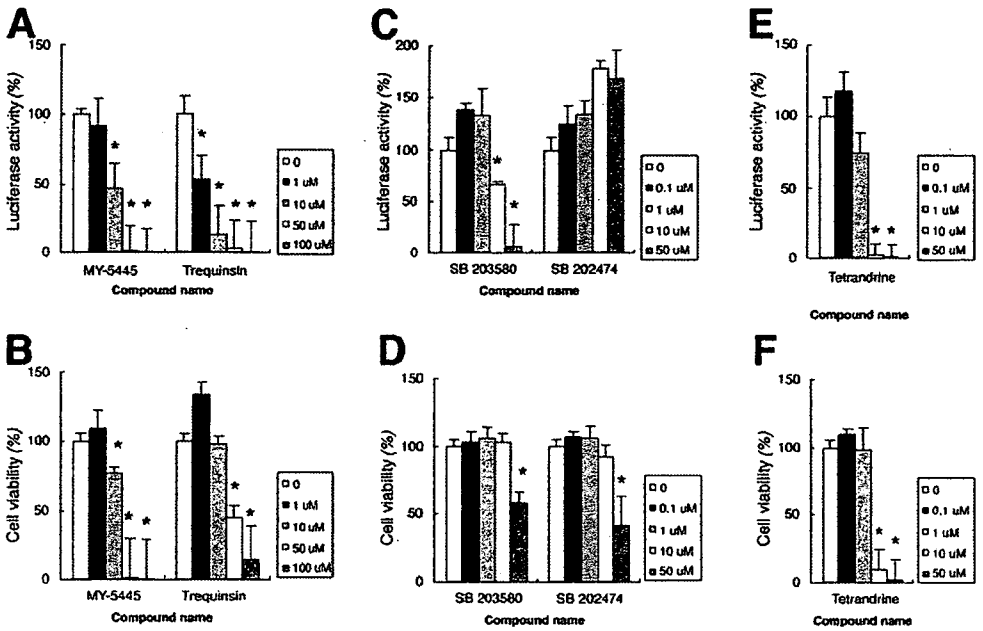

Figure 5. Results of secondary screening with several hit compounds. Luciferase activity for HCV RNA replication levels is shown as a percentage of control (*A, C, E*). Cell viability is also shown as a percentage of control (*B, D, F*). Each *bar* represents the average of triplicate data points with standard deviation represented as the *error bar*. (*A, B*) MY-5445 and trequinsin (*C, D*) SB 203580 (*E, F*) tetrandrine. *Denotes a significant difference from control of at least $P < .05$.

calcium channel blockers, such as verapamil and nifedipine, did not exhibit antiviral activity in either the primary screen or the validation assay (data not shown).

Strikingly, each of the HMG-CoA reductase inhibitors, except for pravastatin, significantly decreased HCV replication in a dose-related manner, with IC_{50} values between 1 and 10 μM. Atorvastatin, simvastatin, and fluvastatin demonstrated strong antiviral effects. Lovastatin, previously reported as an inhibitor of HCV replication,[12] and mevastatin were weakly inhibitory. Lovastatin was significantly cytotoxic at 10, 50, and 100 μM. Mevastatin was not cytotoxic. Pravastatin showed very weak antiviral activity, with only 30% inhibition at 100 μM (Figure 6).

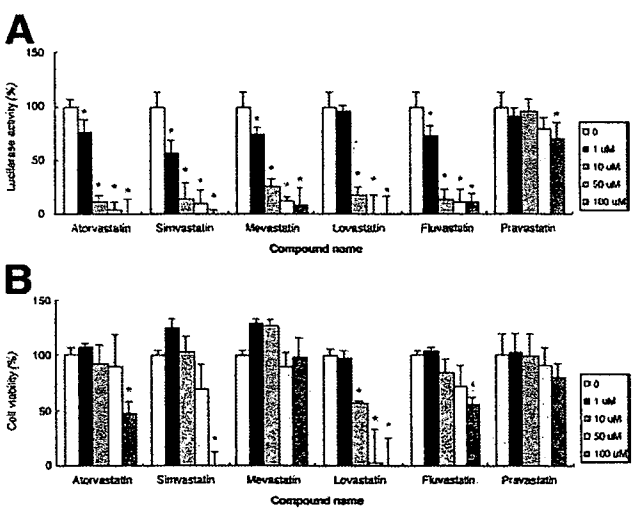

Figure 6. Results of secondary screening with the statins. (*A*) Luciferase activity for HCV RNA replication levels is shown as a percentage of control. (*B*) Cell viability is shown as a percentage of control. Each *bar* represents the average of triplicate data points with standard deviation represented as the *error bar*. *Denotes significant difference from control of at least $P < .05$.

Discussion

Using a subgenomic HCV replicon model, we have established a rapid, reliable, and reproducible cell-based HTS assay system to identify regulators of HCV replication. After first identifying several bioactive small molecules capable of modulating HCV replication in the primary HTS, we verified these hit compounds using a full-length replicon cell line in the secondary validation assay. This method represents an efficient system for the detection of novel compounds, applicable for both academic and pharmaceutical purposes.

In order to successfully develop and execute an efficient, rapid, and reproducible cell-based HTS assay in the field of anti-HCV drug discovery, one must have access to (1) a high-density, automated screening technology platform, (2) a large and diverse collection of appropriate perturbagens, and (3) an accurate and reliable reporter system, which, in this case, was an HCV replicon line that replicates at high levels and harbors a tractable reporter gene.

Traditional HTS techniques using a 96-well plate have been shown to be less efficient at screening very large libraries than more high-density formats. Moreover,